

Mixed State Entanglement Measures in Topological Orders

Chao Yin¹ and Shang Liu^{2,*}

¹*Department of Physics and Center for Theory of Quantum Matter,
University of Colorado, Boulder, Colorado 80309, USA*

²*Kavli Institute for Theoretical Physics, University of California, Santa Barbara, California 93106, USA*

We study two mixed state entanglement measures in topological orders: the so-called *computable cross-norm or realignment* (CCNR) negativity, and the more well-known partial-transpose (PT) negativity, both of which are based on separability criteria. We first compute the CCNR negativity between two spatial regions for tripartite pure states in (2+1)D Chern-Simons (CS) theories using the surgery method, and compare to the previous results on PT negativity. Under certain simplifying conditions, we find general expressions of both mixed state entanglement measures and relate them to the entanglement entropies of different subregions. Then we derive general formulas for both CCNR and PT negativities in the Pauli stabilizer formalism, which is applicable to lattice models in all spatial dimensions. Finally, we demonstrate our results in the \mathbb{Z}_2 toric code model. For tripartitions without trisection points, we provide a strategy of extracting the provably topological and universal terms in both entanglement measures. In the presence of trisection points, our result suggests that the subleading piece in the CCNR negativity is topological, while that for PT is not and depends on the local geometry of the trisections.

Introduction. — There has been a tremendous amount of studies on the entanglement properties of topological orders since the discovery of topological entanglement entropy (EE) [1–4]. In a 2D topologically ordered ground state, the subleading term in the EE of a subregion contains universal information [3–7] and can be used to diagnose the underlying topological phase that lacks conventional order parameters.

As natural generalizations of EE, two spatial regions in a tripartite pure state share entanglement that is often quantified by the partial transpose (PT) negativity \mathcal{E}_{PT} [8, 9]. Such mixed state entanglement measure is also studied in topological orders [10–16]. However, these case-by-case studies work with either specific lattice models, or a continuum theory that is applied to specific tripartitions and quantum states. A general prescription for comparing the continuum and lattice results is also lacking. Moreover, the continuum approach becomes tricky if the tripartition contains a trisection point [15] (i.e., a point where the three parties meet), where the dependence of the subleading term of \mathcal{E}_{PT} on the local trisection geometry is only computed for integer quantum Hall states [16][17].

In this work, we tackle these problems for \mathcal{E}_{PT} together with the less well-known entanglement measure, the *computable cross norm or realignment* (CCNR) negativity [18–20], which is based on a separability criteria similar to PT. For studies of CCNR in other quantum many-body systems, see e.g. Refs. 21–25. We take both a continuum approach using (2+1)D Chern-Simons (CS) theories [26] and a lattice approach using the stabilizer formalism [27]. These two methods are complementary to each other: the former can deal with much more general topologically ordered states in (2+1)D, while the latter applies to all dimensions and to trisection points.

In the continuum, after presenting several concrete examples, we give general formulas for the two negativities for a large class of tripartitions and Wilson line (WL) configurations, including most of the cases in Refs. 12 and 13 as specific examples. On lattices, we derive general formulas for the two entanglement measures in the stabilizer formalism, and apply them to the \mathbb{Z}_2 toric code (TC) model. In the absence of trisection points, we explain how to extract the topological and universal terms in both negativities. For trisection points, the subleading piece in the PT negativity seems to be not topological and depends on the local geometry of trisection. This is in harmonics with a technical problem encountered in the continuum approach. The CCNR negativity, however, is topological and computable in CS theories.

Entanglement and Correlation Measures. — Given a pure state $|\psi\rangle$ shared by two parties A and B , we define the reduced density matrix $\rho_A = \text{Tr}_B(|\psi\rangle\langle\psi|)$, and the Renyi EE $S_A^{(\alpha)} = (1 - \alpha)^{-1} \log \text{Tr}(\rho_A^\alpha)$ which characterizes the entanglement between the two parties. We can further divide A into A_1 and A_2 , and question about the entanglement between them. Let $\{|c\rangle\}$ and $\{|d\rangle\}$ be orthonormal bases of A_1 and A_2 , respectively. We define the partial transposed density matrix $\rho_A^{T_2}$, and a realignment matrix R according to the following equation.

$$\begin{array}{ccc} \begin{array}{c} c \\ \hline \rho_A \\ \hline d \end{array} & \begin{array}{c} c' \\ \hline \rho_A \\ \hline d' \end{array} & \begin{array}{c} c' \\ \hline \rho_A \\ \hline d' \end{array} \\ \hline & \hline & \hline \end{array} \quad \langle c, d | \rho_A | c', d' \rangle = \langle c, d' | \rho_A^{T_2} | c', d \rangle = \langle c', c | R | d', d \rangle \quad (1)$$

The PT and CCNR negativity are then defined as $\mathcal{E}_{\text{PT}} = \log \text{Tr} |\rho_A^{T_2}|$, and $\mathcal{E}_{\text{CCNR}} = \log \text{Tr} \sqrt{R^\dagger R}$, respectively. When ρ_A is separable/unentangled, $\mathcal{E}_{\text{PT}} = 0$ and $\mathcal{E}_{\text{CCNR}} \leq 0$. Therefore, either $\mathcal{E}_{\text{PT}} > 0$ or $\mathcal{E}_{\text{CCNR}} > 0$ implies ρ_A to be entangled, and these two quantities can be regarded as mixed state entanglement measures.

* sliu.phys@gmail.com

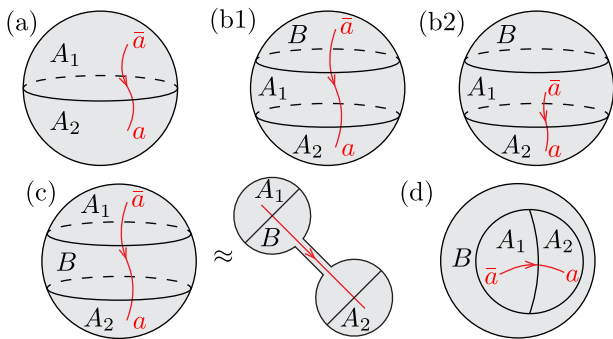


FIG. 1. Wave function $|\psi\rangle$ on a sphere with different partition and WL configurations.

It is known that these two separability criteria are not comparable – neither one is stronger than the other. Both \mathcal{E}_{PT} and $\mathcal{E}_{\text{CCNR}}$ can be computed from replica tricks: $\mathcal{E}_{\text{PT}} = \lim_{m_e \rightarrow 1} \log \text{Tr}[(\rho_A^{T_2})^{m_e}]$ for even m_e , and $\mathcal{E}_{\text{CCNR}} = \lim_{m \rightarrow 1/2} \log \text{Tr}[(R^\dagger R)^m]$ for integer m . The Renyi mutual information $I^{(\alpha)}(A_1, A_2) = S_{A_1}^{(\alpha)} + S_{A_2}^{(\alpha)} - S_A^{(\alpha)}$ is another useful characterization of bipartite correlations. It contains both classical and quantum correlations and hence does not lead to a separability criterion.

Chern-Simons Theories. — We start by computing the negativities using the surgery method in (2+1)D CS theories. A CS theory is a topological gauge theory living in a 3D manifold, producing a state on the 2D surface by path integral. The surface is tripartitioned, and we compute the negativity \mathcal{E}^{top} between A_1 and A_2 . Generically, similar to EE, either negativity for a smooth partition should contain nontopological area-law terms proportional to the lengths of different interface sections [3, 4, 12], together with a topological/universal subleading piece \mathcal{E}^{top} captured by the CS theory. We will discuss later how to deal with these area-law terms and nonsmoothness when comparing with lattice results.

We first present results for several examples, before sketching the derivation and general formulas. Let us first consider states on a sphere. The Hilbert space of a CS theory on a sphere with a pair of dual anyons a, \bar{a} is one-dimensional [26], and the unique state can be prepared by performing the path integral on a solid ball, with an open WL in the representation R_a ending on the surface. Setting a to be trivial corresponds to the case of no anyons. We consider several different partition scenarios as shown in Fig. 1, and the negativities between A_1 and A_2 are given in Table I, where the PT negativity results are mostly directly from Ref. 13. We have denoted by d_a the quantum dimension of the anyon a , and by $\mathcal{D} := \sqrt{\sum_a d_a^2}$ the total quantum dimension of all anyon types. The PT negativity result for the trisection scenario in Fig. 1(d) is absent due to a subtle technical problem [28], which casts doubt on the topological nature of \mathcal{E}_{PT} .

We can analogously compute the negativities for torus states, where topological ground state degeneracy exists:

Case	$\mathcal{E}_{\text{CCNR}}^{\text{top}}$	$\mathcal{E}_{\text{PT}}^{\text{top}}$
a	$\log d_a - \log \mathcal{D}$	$\log d_a - \log \mathcal{D}$
b1	$(\log d_a - \log \mathcal{D})/2$	$\log d_a - \log \mathcal{D}$
b2	$\log d_a - (1/2) \log \mathcal{D}$	$\log d_a - \log \mathcal{D}$
c	$\log \mathcal{D} - \log d_a$	0
d	$\log d_a$	*

TABLE I. Topological CCNR and PT negativities between A_1 and A_2 for the sphere states in Fig. 1, computed by the surgery method of CS theory. Most PT negativity results are directly from Ref. 13. We observe that the CCNR negativity depends on all boundary sections of A_1 and A_2 , not just their interface, as opposed to the PT negativity; for example, compare cases b1 and b2.

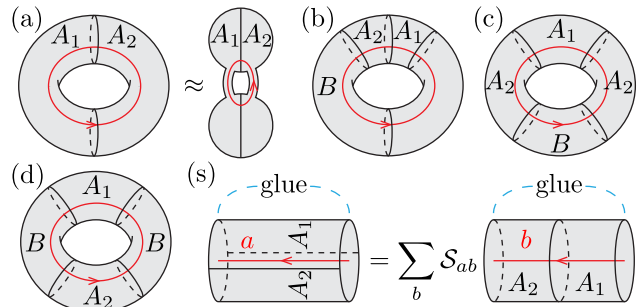


FIG. 2. (a)-(d) Wave function $|\psi\rangle = \sum_j \psi_j |R_j\rangle$ on a torus with different partitions. (e) Effect of the \mathcal{S} transformation.

The Hilbert space on a torus without anyon excitations is multidimensional. An orthonormal basis of the space, denoted as $\{|R_a\rangle\}$, corresponds to a finite set of representations of the gauge group. The state $|R_a\rangle$ can be prepared by performing path integral on the solid torus (bagel) with a noncontractible Wilson loop carrying the corresponding representation R_a inserted; see Fig. 2. It is an eigenstate of Wilson loop operators along the perpendicular direction [6]. We consider a general state $|\psi\rangle = \sum_a \psi_a |R_a\rangle$ with the normalization condition $\sum_a |\psi_a|^2 = 1$. In Table II, we present results on both the CCNR and PT negativities for the tripartitions shown in Fig. 2(a)-(d). Note that the ψ_a dependence is proposed to distinguish abelian and nonabelian topological orders [12, 13].

The results above are calculated by the following procedure [29]. Given the path integral representation of the tripartite state $|\psi\rangle$, we take its mirror image (i.e. reverse

Case	$\mathcal{E}_{\text{CCNR}}^{\text{top}}$	$\mathcal{E}_{\text{PT}}^{\text{top}}$
a	$2 \log(\sum_a \psi_a d_a) - 2 \log \mathcal{D}$	$2 \log(\sum_a \psi_a d_a) - 2 \log \mathcal{D}$
b	0	$\log(\sum_a \psi_a ^2 d_a) - \log \mathcal{D}$
c	$\log(\sum_a \psi_a ^2 d_a) - \log \mathcal{D}$	$\log(\sum_a \psi_a ^2 d_a^2) - 2 \log \mathcal{D}$
d	$\log(\sum_a \psi_a ^2 / d_a^2) + 2 \log \mathcal{D}$	0

TABLE II. Topological CCNR and PT negativities between A_1 and A_2 for the torus states in Fig. 2, computed by the surgery method of CS theory. The PT negativity results are directly from Ref. 13.

the orientation and WL directions) for $\langle \psi |$, and glue the B regions of the two copies together to get the path integral for ρ_A . Then for CCNR (PT similar), we use $2m$ copies of ρ_A and glue them according to $\text{Tr}[(R^\dagger R)^m]$ to get a closed manifold. Its partition function in the replica limit $m \rightarrow 1/2$ then gives $\exp \mathcal{E}_{\text{CCNR}}^{\text{top}}$. To get the partition function, surgery is used to cut the “tubes” of the manifold, so that its topology is simplified to disconnected S^3 s with known partition functions.

This procedure turns out to have universal patterns, which enable calculation for general tripartite state $|\psi\rangle$ satisfying the following assumptions:

- The spacetime manifold has the form of solid balls connected by solid tubes ($D^2 \times [0, 1]$), with at most one circular interface on each ball, and no interface on any tube.
- The WLs can be deformed, without any touching among themselves or between WL endpoints and the interface, to a configuration that all WLs are contained in the 2D surface, and each tube is traversed by the WLs at most once.

The second assumption avoids braiding of WLs during surgery. The first assumption implies that the tripartition interface is a disjoint union of circles that are contractible in the 3D spacetime, and thus there is no trisection points as in Fig. 1(d). All other examples above (Fig. 1(a)-(c) and Fig. 2(a)-(d)) satisfy the two assumptions; in particular, we illustrate the “ball-tube” systems in Fig. 1(c) and Fig. 2(a). Note that it is also possible to consider interfaces made of noncontractible loops, by applying a diffeomorphism on the torus surface, which acts on the Hilbert space as a linear transformation [26]. More concretely, we illustrate in Fig. 2(s) a case where the assumptions are satisfied after the \mathcal{S} transformation, where \mathcal{S}_{ab} is the modular \mathcal{S} matrix [30]. We establish the following result.

Theorem 1. *Consider a CS theory under the above two assumptions with WLs (either closed or open) labeled by w . If each WL carries a definite representation, then the topological entanglement measures satisfy (superscripts “top” omitted)*

$$S_P^{(\alpha)} = -E_P \log \mathcal{D} + \sum_w K_P(w) \log d_{a(w)}, \quad (2)$$

$$\mathcal{E}_{\text{CCNR}}(A_1, A_2) = (S_{A_1}^{(\alpha)} + S_{A_2}^{(\alpha)})/2 - S_A^{(\alpha)}, \quad (3)$$

$$\mathcal{E}_{\text{PT}}(A_1, A_2) = I^{(\alpha)}(A_1, A_2)/2, \quad (4)$$

for arbitrary α . Here in the first line, $P \in \{A_1, A_2, B\}$ is the party, E_P is the number of interfaces shared by P , $K_P(w)$ is the number of interfaces shared by P that WL w traverses, and $a(w)$ is the representation of w .

See SM for results of indefinite representations and the proof. The underlying idea is that gluing replicas and cutting tubes in surgery are both *local* operations: In the ball-tube system, each ball (with its connected tubes) is

operated separately to yield a local factor, and the partition function of the replicated manifold is just the product of all local factors, independent of the *global* topology on which ball is connected to which [31]. We note that Eq. 3 is also satisfied for the tripartition in Fig. 1(d) that does not meet the aforementioned assumptions.

Stabilizer Formalism. — As a complementary approach, we also compute the CCNR and PT negativities in a general Pauli stabilizer state. The results are useful for studying stabilizer lattice models, especially with trisection points. The base of logarithm will be set to 2 for convenience. We consider a state $|\psi\rangle$ uniquely determined by a stabilizer group G . Here, G is an abelian group of (multi-site) Pauli operators with \pm signs such that $-1 \notin G$, and $|\psi\rangle$ is the unique simultaneous eigenstate with eigenvalue $+1$ for all $g \in G$. Let n be the total number of qubits in the Hilbert space. We necessarily have $|G| = 2^n$, and we say the rank, or the number of generators, of G is n .

The EE in a stabilizer state can be conveniently computed [32]. Let A be a subsystem consisting n_A number of qubits, and $G_A \subset G$ be the subgroup of stabilizers inside A . The full and reduced density matrices ρ and ρ_A are respectively given by

$$\rho := |\psi\rangle\langle\psi| = \frac{1}{2^n} \sum_{g \in G} g, \quad \rho_A = \frac{1}{2^{n_A}} \sum_{g \in G_A} g. \quad (5)$$

Let G_A have k generators, or equivalently $|G_A| = 2^k$, then the entropy of subsystem A for any Renyi index is given by $S_A^{(\alpha)} = n_A - k$ [32].

Now we divide subsystem A further into A_1 and A_2 . The CCNR negativity can be computed by expanding each $g \in G_A$ as $g = O^{A_1} \otimes O^{A_2}$ with O^{A_i} acting on A_i . The computation details are given in the SM, and we obtain the following result that agrees with Eq. 3.

Theorem 2. *For a stabilizer state, $\mathcal{E}_{\text{CCNR}}(A_1, A_2) = (S_{A_1}^{(\alpha)} + S_{A_2}^{(\alpha)})/2 - S_A^{(\alpha)}$ for any α .*

To compute the PT negativity, we need more structural knowledge about the stabilizer group. Let k_i be the rank of G_{A_i} . We divide G_A into a product $G_A = G_{A_1} G_{A_2} G_{12}$, where G_{12} has $k - k_1 - k_2$ number of generators independent from those of G_{A_1} and G_{A_2} [33]. Denote by $p_{A_2}(\cdot)$ the restriction of a stabilizer to subsystem A_2 , which is well defined up to a sign if we require the corresponding restriction to be hermitian. According to Ref. 32 (in particular Lemma 2), we have the following canonical choice of the generators of G_{12} :

$$G_{12} = \langle z_1, \dots, z_r, w_1, \dots, w_s, \bar{w}_1, \dots, \bar{w}_s \rangle, \quad (6)$$

such that $p_{A_2}(z_i)$ commutes with all generators of G_{12} (therefore commutes with G_A), and $p_{A_2}(w_i)$ commutes with all generators of G_{12} except for \bar{w}_i (therefore the same holds if w_i and \bar{w}_i are exchanged). We can always choose the signs of $p_{A_2}(\cdot)$ to preserve the group multiplication laws. Then $p_{A_2}(G_{12})$ forms a group, and the

integer r appearing in Eq. 6 is nothing but the rank of its center. With Eq. 6 in mind, the PT negativity of a stabilizer state can be computed as detailed in the SM, and we obtain the following result.

Theorem 3. *For a stabilizer state, $\mathcal{E}_{\text{PT}}(A_1, A_2) = s = [I^{(\alpha)}(A_1, A_2) - r]/2$ for any α .*

As we will see, with trisection points, the dependence of r on local geometry is exactly the reason why the subleading term in \mathcal{E}_{PT} is nontopological.

Lattice Examples. — Let us demonstrate our results in lattice examples. In order to compare with the continuum results, we need to first precisely define the subleading term \mathcal{E}^{top} of each negativity \mathcal{E} on lattices. Considering that $A_1 A_2$ interfaces and $A_i B$ interfaces contribute differently to either negativity \mathcal{E} , we define the following linear combination to cancel both types of area-law terms:

$$\Delta := \mathcal{E}(A_1, A_2) - \mathcal{E}(A, \emptyset) - [\mathcal{E}(A_1, \bar{A}_1) + \mathcal{E}(A_2, \bar{A}_2) - \mathcal{E}(A, B)]/2, \quad (7)$$

where $\bar{\cdot}$ means complement. The terms except the first one are actually EEs: $\mathcal{E}_{\text{CCNR}}(A, \emptyset) = -S_A^{(2)}/2$, $\mathcal{E}_{\text{PT}}(A, \emptyset) = 0$, and $\mathcal{E}(P, \bar{P}) = S_P^{(1/2)}$. Thus we can compute $\mathcal{E}^{\text{top}}(A_1, A_2)$ from the lattice result of Δ and topological EEs by adding a superscript “top” to each term on the right-hand side of Eq. 7.

An immediate question is whether \mathcal{E}^{top} defined this way is topological (insensitive to smooth deformations of the subregions) and universal (insensitive to perturbations to the Hamiltonian). There may be problems associated with corners and the trisection points. In the absence of trisections points, suppose all nontopological/nonuniversal terms in \mathcal{E} are made of *local* contributions near the interfaces that are insensitive to changes far away, then all these terms have been cancelled out in Δ (see also the argument in Ref. 3). Δ and \mathcal{E}^{top} are thus *topological and universal*, even for nonsmooth interfaces. However, in the presence of trisection points, the interfaces between different pairs of subregions meet together, and there may be uncanceled local contributions near the trisections. We need to study concrete examples to see whether \mathcal{E}^{top} is robust in this situation.

Let us consider the \mathbb{Z}_2 TC model [34], the simplest lattice model with a topological order. The model can be defined on an arbitrary 2D closed space manifold discretized into a lattice with qubits living on links. The Hamiltonian takes the form

$$H_{\text{TC}} = - \sum_s \mathbf{Z}_s - \sum_p \mathbf{X}_p, \quad (8)$$

where \mathbf{Z}_s is the product of Pauli Z operators on all links containing the site s , and \mathbf{X}_p is the product of Pauli X operators on all links surrounding the plaquette p ; see Fig. 3(a) for the example of a square lattice. For concreteness, we put the model on a cube surface (topologically a sphere) as shown in Fig. 3(b), and focus on its unique ground state.

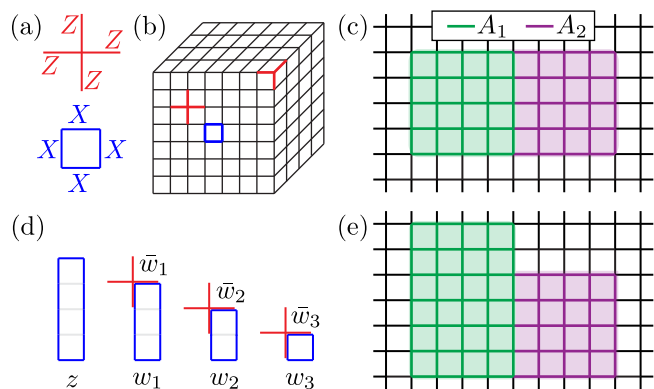


FIG. 3. (a) Star and plaquette terms of the toric code model in the case of square lattice. (b) Toric code on a cube surface which is topologically a sphere. (c) Subsystems A_1 (green, left) and A_2 (purple, right). (d) Canonical generators of G_{12} . (e) A deformation of the tripartition in panel c.

As the first example, consider the tripartition in Fig. 1(b). We can prove $r = 0$ in this case: If $r > 0$, $p_{A_2}(z_1)$ commutes with G_A . Since $p_{A_2}(z_1)$ lies in A_2 and is far away from the AB interface, it should then commute with all star and plaquette terms. Now suppose we replace B by A_1 , the *old* z_1 still satisfies $z_1 \notin G_{A_1} G_{A_2}$ and $p_{A_2}(z_1)$ commuting with G_A , thus $r > 0$ still holds, but this is not possible because $\mathcal{E}_{\text{PT}}(A_1, A_2) = I^{(1/2)}(A_1, A_2)/2$ for a bipartite pure state. Hence, by comparing Theorem 1, 2, and 3, we see that $\mathcal{E}_{\text{PT}}^{\text{top}}$ and $\mathcal{E}_{\text{CCNR}}^{\text{top}}$ computed on the lattice indeed match with the continuum results.

Next, we consider A_1 and A_2 to be adjacent rectangular regions as shown in Fig. 3(c); this corresponds to the tricky scenario in Fig. 1(d). Any stabilizer of the system, to commute with the star and plaquette terms, must consist of X loops along links, and Z loops along dual lattice links. One can then check that a set of independent generators for G_A is simply all star and plaquette terms inside, similarly for G_{A_1} and G_{A_2} . Let L_{A_1} , L_{A_2} , and L_A be the lattice perimeters of A_1 , A_2 , and A , respectively. A simple counting gives $S_A^{(\alpha)} = n_A - k = L_A - 1$, similarly for A_1 and A_2 . Note that the -1 is nothing but the topological EE of a contractible region with a smooth boundary for the TC model [3, 4]. The rank of G_{12} is given by $k - k_1 - k_2 = 2L_{12} - 1 = I^{(\alpha)}(A_1, A_2)$ where L_{12} is the lattice length of the interface between A_1 and A_2 . We can choose the generators of G_{12} to be the star and plaquette terms crossing the interface, but they do not satisfy the property of canonical generators introduced previously. We show in Fig. 3(d) how these generators can be reorganized into a canonical set, from which we see $r = 1$. According to Theorem 3, $\mathcal{E}_{\text{PT}}(A_1, A_2) = [I^{(\alpha)}(A_1, A_2) - 1]/2 = L_{12} - 1$. The CCNR negativity is found to be $\mathcal{E}_{\text{CCNR}}(A_1, A_2) = L_{12} - L_A/2$. From our previous lattice definition of \mathcal{E}^{top} , we obtain $\mathcal{E}_{\text{PT}}^{\text{top}} = -1$ and $\mathcal{E}_{\text{CCNR}}^{\text{top}} = 0$, where the latter is consistent

with the field-theoretic calculation.

In view of Theorem 2, the above result of $\mathcal{E}_{\text{CCNR}}^{\text{top}}$ should at least be topological, but $\mathcal{E}_{\text{PT}}^{\text{top}}$ is more subtle. Consider the deformed tripartition in Fig. 3(e). With one more star term included in G_{12} , we see $r = 0$, and therefore $\mathcal{E}_{\text{PT}} = I^{(\alpha)}(A_1, A_2)/2$. It follows that $\mathcal{E}_{\text{PT}}^{\text{top}}$ now becomes $-1/2$, different from the previous -1 result. Hence, $\mathcal{E}_{\text{PT}}^{\text{top}}$ defined according to Eq. 7 is actually not topological.

In the SM, we provide one more example on torus without trisection points.

Discussions. — Future works are needed to check whether our result of $\mathcal{E}_{\text{CCNR}}^{\text{top}}$ in the presence of trisection points has any universal meaning on lattices. See Refs. 35 and 15 for related discussions on the so-called *reflected entropy*. Behaviors of both negativities in string-net models and (3+1)D systems are also interesting to explore. 1

Acknowledgments. — We are grateful to Yuhan Liu for a stimulating discussion, and to Jonah Kudler-Flam, Shinsei Ryu, and Ashvin Vishwanath for valuable feedbacks on our manuscript. S. L. is supported by the Gordon and Betty Moore Foundation under Grant No. GBMF8690 and the National Science Foundation under Grant No. NSF PHY-1748958.

Note added. — Upon completion of this manuscript, we became aware of a few related works: The use of PT negativity for diagnosing error-corrupted topological orders is discussed in Ref. 36. Refs. 37 and 38 both have continuum computations of PT negativity with trisection points. The former takes an anyon diagram approach with a particular regularization of the trisection points (wormholes), and the latter takes a boundary/vertex state approach.

-
- [1] A. Hamma, R. Ionicioiu, and P. Zanardi, Ground state entanglement and geometric entropy in the Kitaev model [rapid communication], *Physics Letters A* **337**, 22 (2005), [arXiv:quant-ph/0406202 \[quant-ph\]](#).
- [2] A. Hamma, R. Ionicioiu, and P. Zanardi, Bipartite entanglement and entropic boundary law in lattice spin systems, *Phys. Rev. A* **71**, 022315 (2005), [arXiv:quant-ph/0409073 \[quant-ph\]](#).
- [3] A. Kitaev and J. Preskill, Topological Entanglement Entropy, *Phys. Rev. Lett.* **96**, 110404 (2006), [arXiv:hep-th/0510092 \[hep-th\]](#).
- [4] M. Levin and X.-G. Wen, Detecting Topological Order in a Ground State Wave Function, *Phys. Rev. Lett.* **96**, 110405 (2006), [arXiv:cond-mat/0510613 \[cond-mat.str-el\]](#).
- [5] S. Dong, E. Fradkin, R. G. Leigh, and S. Nowling, Topological entanglement entropy in Chern-Simons theories and quantum Hall fluids, *Journal of High Energy Physics* **2008**, 016 (2008), [arXiv:0802.3231 \[hep-th\]](#).
- [6] Y. Zhang, T. Grover, A. Turner, M. Oshikawa, and A. Vishwanath, Quasiparticle statistics and braiding from ground-state entanglement, *Phys. Rev. B* **85**, 235151 (2012), [arXiv:1111.2342 \[cond-mat.str-el\]](#).
- [7] T. Grover, Y. Zhang, and A. Vishwanath, Entanglement entropy as a portal to the physics of quantum spin liquids, *New Journal of Physics* **15**, 025002 (2013), [arXiv:1302.0899 \[cond-mat.str-el\]](#).
- [8] A. Peres, Separability Criterion for Density Matrices, *Phys. Rev. Lett.* **77**, 1413 (1996), [arXiv:quant-ph/9604005 \[quant-ph\]](#).
- [9] G. Vidal and R. F. Werner, Computable measure of entanglement, *Phys. Rev. A* **65**, 032314 (2002), [arXiv:quant-ph/0102117 \[quant-ph\]](#).
- [10] Y. A. Lee and G. Vidal, Entanglement negativity and topological order, *Phys. Rev. A* **88**, 042318 (2013), [arXiv:1306.5711 \[quant-ph\]](#).
- [11] C. Castelnovo, Negativity and topological order in the toric code, *Phys. Rev. A* **88**, 042319 (2013), [arXiv:1306.4990 \[cond-mat.str-el\]](#).
- [12] X. Wen, S. Matsuura, and S. Ryu, Edge theory approach to topological entanglement entropy, mutual information, and entanglement negativity in Chern-Simons theories, *Phys. Rev. B* **93**, 245140 (2016), [arXiv:1603.08534 \[cond-mat.mes-hall\]](#).
- [13] X. Wen, P.-Y. Chang, and S. Ryu, Topological entanglement negativity in Chern-Simons theories, *Journal of High Energy Physics* **2016**, 12 (2016), [arXiv:1606.04118 \[cond-mat.str-el\]](#).
- [14] P. K. Lim, H. Asasi, J. C. Y. Teo, and M. Mulligan, Disentangling (2 + 1)D topological states of matter with entanglement negativity, *Phys. Rev. B* **104**, 115155 (2021), [arXiv:2106.07668 \[cond-mat.str-el\]](#).
- [15] Y. Liu, R. Sohal, J. Kudler-Flam, and S. Ryu, Multipartitioning topological phases by vertex states and quantum entanglement, *Phys. Rev. B* **105**, 115107 (2022), [arXiv:2110.11980 \[cond-mat.str-el\]](#).
- [16] C.-C. Liu, J. Geoffrion, and W. Witczak-Krempa, Entanglement negativity versus mutual information in the quantum Hall effect and beyond, *arXiv e-prints*, [arXiv:2208.12819 \(2022\)](#), [arXiv:2208.12819 \[cond-mat.str-el\]](#).
- [17] See also Refs. 39 and 40 for corner contributions to EE.
- [18] O. Rudolph, Further results on the cross norm criterion for separability, *Quantum Information Processing* **4**, 219 (2005), [arXiv:quant-ph/0202121 \[quant-ph\]](#).
- [19] K. Chen and L.-A. Wu, A matrix realignment method for recognizing entanglement, *arXiv e-prints*, [quant-ph/0205017 \(2002\)](#), [arXiv:quant-ph/0205017 \[quant-ph\]](#).
- [20] O. Rudolph, Some properties of the computable cross-norm criterion for separability, *Phys. Rev. A* **67**, 032312 (2003), [arXiv:quant-ph/0212047 \[quant-ph\]](#).
- [21] G. Aubrun and I. Nechita, Realigning random states, *Journal of Mathematical Physics* **53**, 102210 (2012), [arXiv:1203.3974 \[math.PR\]](#).
- [22] B. Collins and I. Nechita, Random matrix techniques in quantum information theory, *Journal of Mathematical Physics* **57**, 015215 (2016), [arXiv:1509.04689 \[quant-ph\]](#).
- [23] C. Yin and Z. Liu, Universal entanglement and correlation measure in two-dimensional conformal field theory, *arXiv e-prints*, [arXiv:2211.11952 \(2022\)](#), [arXiv:2211.11952 \[cond-mat.stat-mech\]](#).
- [24] Z. Liu, Y. Tang, H. Dai, P. Liu, S. Chen, and X. Ma,

- Detecting entanglement in quantum many-body systems via permutation moments, *Phys. Rev. Lett.* **129**, 260501 (2022).
- [25] A. Milekhin, P. Rath, and W. Weng, Computable Cross Norm in Tensor Networks and Holography, arXiv e-prints , arXiv:2212.11978 (2022), arXiv:2212.11978 [hep-th].
- [26] E. Witten, Quantum field theory and the Jones polynomial, *Communications in Mathematical Physics* **121**, 351 (1989).
- [27] M. A. Nielsen and I. L. Chuang, *Quantum Computation and Quantum Information: 10th Anniversary Edition* (Cambridge University Press, 2010).
- [28] With the replica approach, one encounters topological spaces that are not manifolds – suspensions of tori with many handles. Thus the surgery method does not apply here.
- [29] We refer to supplemental material (SM) and [13] for pedagogical overview on the surgery method.
- [30] S matrix is defined both in the theory of anyons [41, 42] and in rational conformal field theories [43]. CS theories connect these two contexts together.
- [31] Strictly speaking, one needs to deal with an extra summation over representations in the general case; see SM.
- [32] D. Fattal, T. S. Cubitt, Y. Yamamoto, S. Bravyi, and I. L. Chuang, Entanglement in the stabilizer formalism, arXiv e-prints , quant-ph/0406168 (2004), arXiv:quant-ph/0406168 [quant-ph].
- [33] The choice of G_{12} is in general not unique.
- [34] A. Y. Kitaev, Fault-tolerant quantum computation by anyons, *Annals of Physics* **303**, 2 (2003), arXiv:quant-ph/9707021 [quant-ph].
- [35] K. Siva, Y. Zou, T. Soejima, R. S. K. Mong, and M. P. Zaletel, Universal tripartite entanglement signature of ungappable edge states, *Phys. Rev. B* **106**, L041107 (2022), arXiv:2110.11965 [quant-ph].
- [36] R. Fan, Y. Bao, E. Altman, and A. Vishwanath, Diagnostics of mixed-state topological order and breakdown of quantum memory, arXiv e-prints , arXiv:2301.05689 (2023), arXiv:2301.05689 [quant-ph].
- [37] R. Sohal and S. Ryu, Entanglement in Tripartitions of Topological Orders: A Diagrammatic Approach, in preparation.
- [38] Y. Liu, Y. Kusuki, J. Kudler-Flam, R. Sohal, and S. Ryu, Multipartite entanglement in two-dimensional chiral topological liquids, arXiv e-prints , arXiv:2301.07130 (2023).
- [39] I. D. Rodríguez and G. Sierra, Entanglement entropy of integer quantum Hall states in polygonal domains, *Journal of Statistical Mechanics: Theory and Experiment* **2010**, 12033 (2010), arXiv:1007.5356 [cond-mat.str-el].
- [40] B. Sirois, L. M. Fournier, J. Leduc, and W. Witczak-Krempa, Geometric entanglement in integer quantum Hall states, *Phys. Rev. B* **103**, 115115 (2021).
- [41] A. Kitaev, Anyons in an exactly solved model and beyond, *Annals of Physics* **321**, 2 (2006), arXiv:cond-mat/0506438 [cond-mat.mes-hall].
- [42] P. H. Bonderson, *Non-Abelian Anyons and Interferometry*, Ph.D. thesis, California Institute of Technology (2012).
- [43] P. Di Francesco, P. Mathieu, and D. Sénéchal, *Conformal field theory* (Springer Science & Business Media, 2012).

SUPPLEMENTAL MATERIAL: Mixed State Entanglement Measures in Topological Orders

CONTENTS

I. Entanglement Measures in Chern-Simons Theory	7
A. overview	7
1. tripartition: ball-tube system	7
2. assumption on WL	8
3. entanglement measures and the replica method	9
4. main result	10
5. surgery method: overview and an example	10
B. no Wilson line	12
1. trace over B	12
2. replica method for EE and PT	13
3. replica method for CCNR	14
C. normalization with Wilson line: extra factor for party balls	14
1. only one WL, which traverses each ball at most once	14
2. multiple WLs, where each WL can traverse a ball multiple times	15
D. Wilson line contribution to entanglement	16
1. WL in an edge ball that traverses the interface	16
2. WL in a party ball	17
3. WL in an edge ball that does not traverse the interface	19
4. GEF for only one WL, which traverses each ball at most once	19
5. general case: factorization property	19
II. Entanglement Measures in Stabilizer Formalism	20
A. CCNR in stabilizer formalism	20
B. PT in stabilizer formalism	20
C. one more toric code example	21

I. ENTANGLEMENT MEASURES IN CHERN-SIMONS THEORY

A. overview

Let \mathcal{M} be an orientable closed 2D manifold with genus $g \geq 0$. Consider a Chern-Simons (CS) theory on \mathcal{M} and its specific state $|\psi\rangle$, defined by the path integral in the 3D interior $\mathcal{M}_3 \supset \mathcal{M}$ of \mathcal{M} with Wilson lines (WLs) inserted. The goal of this paper is to calculate entanglement measures of $|\psi\rangle$ with respect to a partition of \mathcal{M} under fairly general assumptions. In this overview subsection we set up the problem, present our main results, and finally review the surgery method that we will use with an example.

1. tripartition: ball-tube system

Consider a tripartition $\mathcal{M} = A_1 \cup A_2 \cup B$ that separates \mathcal{M} into regions $\{r_j : j = 1, \dots, N\}$, where each region r_j belongs to either party A_1, A_2 or B . This reduces to a bipartition $\mathcal{M} = A \cup B$ when combining $A = A_1 \cup A_2$. We make an assumption on the tripartition:

Assumption 1. *The edges of the regions $\{r_j\}$ are disjoint circles that are contractable in \mathcal{M}_3 .*

In particular, this implies that no three different regions i, j, k share common points:

$$r_i \cap r_j \cap r_k = \emptyset. \tag{S1}$$

Any pair of regions (r_i, r_j) either is not connected, or shares ≥ 1 disconnected edges. All edges do not touch each other according to (S1). Beyond (S1), Assumption 1 also requires contractability of edges in the bulk. For example,

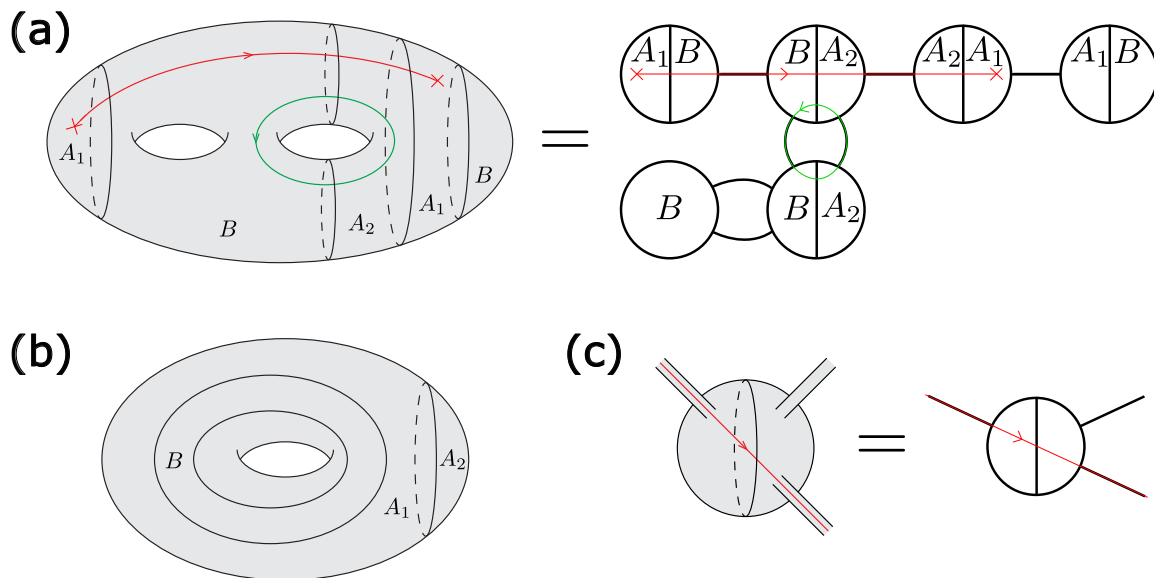


FIG. S1. (a) A tripartition of a genus-2 surface \mathcal{M} that satisfies Assumption 1, which is deformed to the right ball-tube system. The relevant quantities are $E = 5, E_B = 4, K(1) = 3, K_B(1) = 2, K_{12}(1) = K_{1B}(1) = K_{2B}(1) = 1, K(2) = K_{2B}(2) = 2, K_{12}(2) = 0$. (b) A tripartition that violates Assumption 1, which cannot be deformed to a ball-tube system. (c) The 3D version of an example element in the sketched ball-tube system (a). In particular, a black line represents a tube with cross section D^2 , and a red line is a WL.

Fig. S1(a) and any tripartition on the sphere that satisfies (S1) fulfil Assumption 1, while Fig. S1(b) does not: the edge circles between B and A_1 are non-contractable. Note that tripartitions like Fig. S1(b) can be transformed using modular transformation to a “good” tripartition satisfying Assumption 1, with suitable Wilson loops inserted [12]. However, we leave as an open question whether any tripartition satisfying (S1) can be transformed in this way, and just assume Assumption 1 throughout.

Based on Assumption 1, \mathcal{M}_3 can be deformed to a ball-tube system, with Fig. S1(a) as an example. In the ball-tube system, each region r_j on the surface corresponds to an interior 3D region \mathcal{R}_j , composed of several balls and half-balls connected by D^2 -tubes. Here a (half-)ball is topologically D^3 while a D^2 -tube is $D^2 \times [0, 1]$. To connect regions, for each edge between r_i and r_j , the corresponding half-ball of \mathcal{R}_i combines with its counterpart half-ball of \mathcal{R}_j to make a ball. We refer to this as an *edge ball* to differentiate with the *party balls* that belong to only one party, and we call the joint surface between the two half-balls an *interface*. The boundary of the interface is then an edge that connects r_i and r_j . In this way \mathcal{M}_3 is deformed to a set \mathcal{B} of balls connected by tubes.

We provide further justification on why the above deformation is possible. Namely, one can start from the unpartitioned \mathcal{M}_3 and add the edges one by one. The initial \mathcal{M}_3 is naturally a ball-tube system, where a central ball is connected to g surrounding balls by two D^2 -tubes each. When adding the first edge that is contractable in \mathcal{M}_3 , one of the balls will be cut by an interface to become an edge ball. We do not need to make the cut on tubes because it can always deform to one ball on its end. Then adding the second edge, there are two possibilities: if the cut is on a party ball then it becomes an edge ball just as step one; otherwise if the cut is on an edge ball, we deform the ball to two edge balls connected by one new tube. The manifold thus remains to be a ball-tube system, so that edges can be added one by one.

There is some freedom in the above procedure, namely for each \mathcal{R}_j , which pairs of (half-)balls are connected by tubes? The entanglement quantities we study should not depend on the choice. Therefore, to express our results, we need to use quantities that do not depend on the connection. Define E to be the total number of edges, which is just the number of edge balls independent of the connection. Moreover, define E_P ($P = A_1, A_2, B$) to be the number of edges with party P on one side. We will define similar quantities for WL in the next subsection.

2. assumption on WL

Let W WLs be embedded in \mathcal{M}_3 . A WL can either be a loop in the interior, or puncture the surface \mathcal{M} with two anyons. To avoid braiding and knot, we consider the following WL configuration in the ball-tube system \mathcal{M}_3 :

Assumption 2. *The WLs can be simultaneously deformed, without touching among themselves or between WL endpoints and edges on the surface \mathcal{M} , to a configuration that all WLs are contained in the surface \mathcal{M} and do not touch each other. Moreover, each D^2 -tube contains at most one WL which goes through the tube once.*

The deformation does not change topology, and thus does not change the quantities that we will compute. Moreover, contractable (in \mathcal{M}_3) Wilson loops with no flux of other WLs can be annihilated freely, as one can check explicitly using surgery introduced in Section IA 5. Note that even if a tube contains more than one WLs in one ball-tube system representation of \mathcal{M}_3 , one may adjust the connection of balls to get another ball-tube system that satisfies Assumption 2. From now on we assume such a ball-tube system is chosen. Similar to E , the number of interfaces traversed by the WL w , $K(w)$, is well-defined. Note that an interface can contribute more than one to $K(w)$, if it is traversed by w back and forth. Similarly, $K_P(w)$ ($K_{PP'}(w)$) counts the number of interfaces shared by party P (and party P') that w traverses.

Each WL is assigned a representation a , and we consider the superposition

$$|\psi\rangle = \sum_{a(1)\cdots a(W)} \psi_{a(1)}(1) \times \psi_{a(2)}(2) \times \cdots \times \psi_{a(W)}(W) |a(1)\cdots a(W)\rangle. \quad (\text{S2})$$

Here $|a(1)\cdots a(W)\rangle$ is the *normalized* state with each WL $w \in \{1, \dots, W\}$ in the fixed representation $a(w)$. As we will check in Section IC, these states are orthogonal to each other. Thus (S2) can be viewed as a direct product among WLs, and we assume $\sum_a |\psi_a(w)|^2 = 1$ for any w such that $\langle\psi|\psi\rangle = 1$.

3. entanglement measures and the replica method

We study three entanglement measures. First, $|\psi\rangle$ is a bipartite pure state shared by A and B , so there is entanglement entropy (EE) from the reduced density matrix ρ_A on A

$$S_A = S_B = -\text{Tr}(\rho_A \log \rho_A) = \lim_{n \rightarrow 1} S_A^{(n)}, \quad \text{where} \quad S_A^{(n)} = \frac{1}{1-n} \log \text{Tr}(\rho_A^n). \quad (\text{S3})$$

Here $S_A^{(n)}$ is the n -th Rényi EE. In the replica method, we will compute $S_A^{(n)}$ first, and then take the replica limit $n \rightarrow 1$ to get the von Neumann EE. The same method is also applied for the following two entanglement measures.

ρ_A is a bipartite mixed state shared by A_1 and A_2 , and we study two quantities that measure the quantum correlation between the two parties: the partial transpose negativity (PT) \mathcal{E}_{PT} , and the computable cross norm negativity (CCNR) $\mathcal{E}_{\text{CCNR}}$ [19]. They are defined by

$$\mathcal{E}_{\text{PT}} = \log \left\| \rho_A^{T_2} \right\|_1 = \lim_{\text{even } n \rightarrow 1} \mathcal{E}_{\text{PT}}^{(n)}, \quad \text{where} \quad \mathcal{E}_{\text{PT}}^{(n)} = \log \text{Tr} \left(\rho_A^{T_2} \right)^n, \quad (\text{S4a})$$

$$\mathcal{E}_{\text{CCNR}} = \log \|R_\rho\|_1 = \lim_{\text{even } n \rightarrow 1} \mathcal{E}_{\text{CCNR}}^{(n)}, \quad \text{where} \quad \mathcal{E}_{\text{CCNR}}^{(n)} = \log \text{Tr} \left(R_\rho^\dagger R_\rho \right)^{n/2}. \quad (\text{S4b})$$

Here T_2 means partial transpose on A_2 , and R_ρ is related to ρ by

$$\langle e_1 | \langle e'_1 | R_\rho | e_2 \rangle | e'_2 \rangle = \langle e_1 | \langle e_2 | \rho | e'_1 \rangle | e'_2 \rangle, \quad (\text{S5})$$

where $\{|e_1\rangle\}, \{|e_2\rangle\}$ are basis for subsystem A_1 and A_2 respectively.

4. main result

For any state (S2) with Assumptions 1 and 2, we have

$$S_A = -E_B \log \mathcal{D} + \sum_w \sum_a |\psi_a(w)|^2 \left(K_B(w) \log d_a - \mathbb{I}[K_B(w) > 0] \log |\psi_a(w)|^2 \right), \quad (\text{S6a})$$

$$\mathcal{E}_{\text{PT}} = -(E - E_B) \log \mathcal{D} + \sum_w \begin{cases} \log \left(\sum_a |\psi_a(w)|^2 d_a^{K(w) - K_B(w)} \right), & \text{if } K_B(w) > 0 \\ 2 \log \left(\sum_a |\psi_a(w)| d_a^{K(w)/2} \right), & \text{if } K(w) > K_B(w) = 0 \end{cases} \quad (\text{S6b})$$

$$\begin{aligned} \mathcal{E}_{\text{CCNR}} &= -(E - \frac{3}{2}E_B) \log \mathcal{D} \\ &+ \sum_w \begin{cases} \log \left(\sum_a |\psi_a(w)|^2 d_a^{K(w) - \frac{3}{2}K_B(w)} \right), & \text{if at least two in } \{K_{12}(w), K_{1B}(w), K_{2B}(w)\} \text{ are nonzero} \\ \frac{1}{2} \log \left(\sum_a |\psi_a(w)|^4 d_a^{-K(w)} \right), & \text{if only one in } \{K_{1B}(w), K_{2B}(w)\} \text{ is nonzero and } K_{12}(w) = 0 \\ 2 \log \left(\sum_a |\psi_a(w)| d_a^{K(w)/2} \right), & \text{if } K(w) > K_B(w) = 0 \end{cases} \end{aligned} \quad (\text{S6c})$$

where $\mathcal{D} = 1/S_{00}$ with S_{ab} being the modular \mathcal{S} matrix of the Chern-Simons theory, and

$$d_a = S_{0a}/S_{00}, \quad (\text{S7})$$

is the quantum dimension.

When all representations are fixed $\psi_a(w) = \delta_{a,a(w)}$ by some function $a(w)$, we have simplified expressions for all Rényi quantities

$$S_P^{(n)} = S_P = -E_P \log \mathcal{D} + \sum_w K_P(w) \log d_{a(w)}, \quad (\text{S8a})$$

$$\mathcal{E}_{\text{PT}}^{(n)} = -[E - E_B + E(1 - n)] \log \mathcal{D} + \sum_w [K(w) - K_B(w) + K(w)(1 - n)] \log d_{a(w)}, \quad (\text{S8b})$$

$$\begin{aligned} \mathcal{E}_{\text{CCNR}}^{(n)} &= - \left[E - \frac{3}{2}E_B + \left(E - \frac{1}{2}E_B \right) (1 - n) \right] \log \mathcal{D} \\ &+ \sum_w \left[K(w) - \frac{3}{2}K_B(w) + \left(K(w) - \frac{1}{2}K_B(w) \right) (1 - n) \right] \log d_{a(w)}, \end{aligned} \quad (\text{S8c})$$

which reduces to

$$2 \mathcal{E}_{\text{PT}}^{(n)} = S_1 + S_2 - S_{12} + (1 - n)(S_1 + S_2 + S_{12}) = I_{12} + (1 - n)(S_1 + S_2 + S_{12}), \quad (\text{S9a})$$

$$2 \mathcal{E}_{\text{CCNR}}^{(n)} = S_1 + S_2 - 2S_{12} + (1 - n)(S_1 + S_2) = 2 \mathcal{E}_{\text{PT}}^{(n)} - (2 - n)S_{12}, \quad (\text{S9b})$$

where $S_{12} = S_A = S_B$, and I_{12} is the mutual information shared between A_1 and A_2 .

5. surgery method: overview and an example

Surgery is introduced in [26] to calculate partition functions of Chern-Simons theories in general settings (with braiding among WLS etc). For our purpose, we only need two gadgets:

1. The partition function of a S^3 with a single Wilson loop of representation a in it is

$$Z_a = S_{0a}. \quad (\text{S10})$$

2. As shown in Fig. S2(a), an S^2 -tube traversed by two WLS of representation a can be cut by a S^3 with a Wilson loop of the same representation a in it. Formally, let M be the original manifold with the S^2 -tube connected, and let M_L, M_R be the two manifolds after cutting the tube (and reconnecting the cutted WL in each manifold), then

$$Z(M) \cdot Z_a = Z(M_L) \cdot Z(M_R). \quad (\text{S11})$$

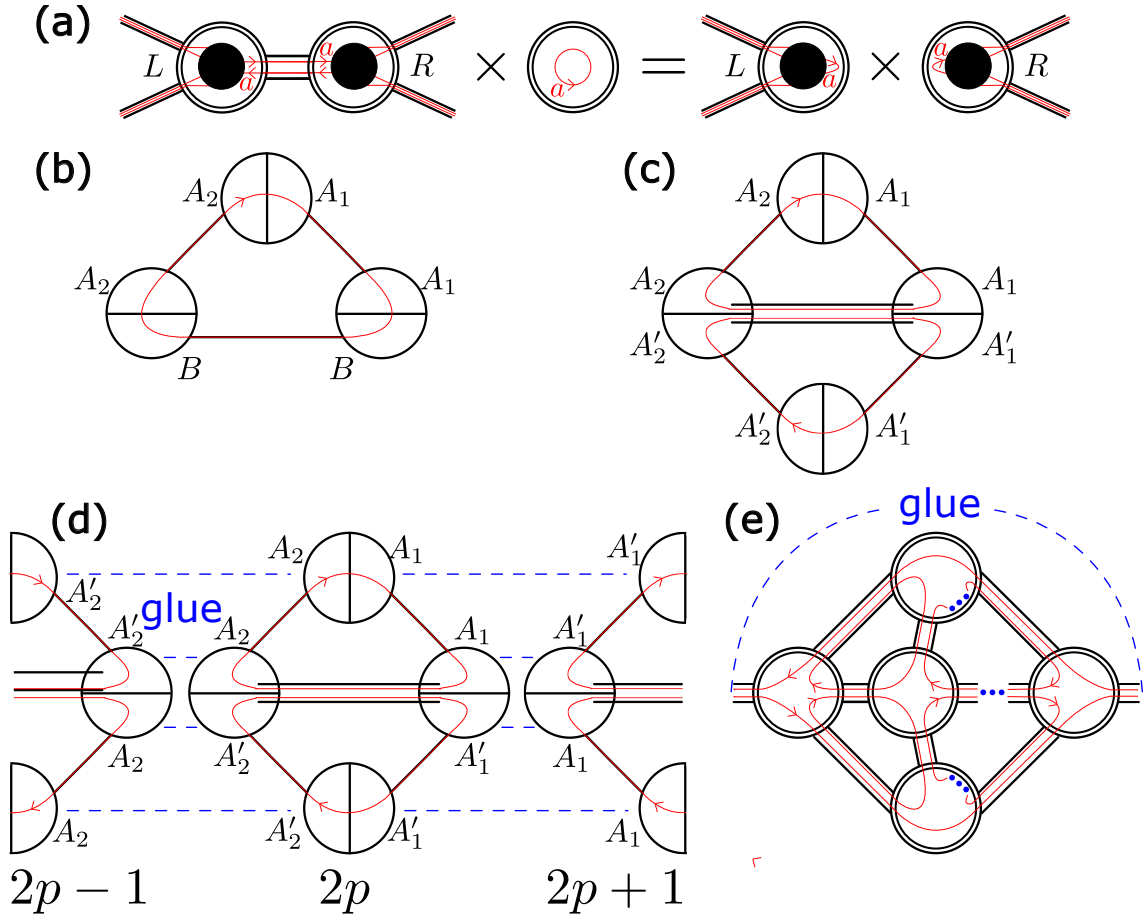


FIG. S2. (a) In the surgery method, an S^2 -tube traversed by two WLs of representation a is cut by a S^3 with a Wilson loop of the same representation a in it. The case where no WL traverses the tube is just setting $a = 0$. In comparison to Fig. S1, two black concentric circles represent a S^3 , while two black parallel straight lines represent a S^2 -tube. The black solid circle means the structure of WLs inside does not matter. L, R means the number of tubes going out of the left/right S^3 , while only two of the tubes are explicitly shown. (b-e) Calculation of CCNR for Fig. 2(b) in the main text. (b) The ball-tube representation of $|\psi\rangle$. (c) The path integral representation of ρ_A . (d) The way to glue n copies of ρ_A together to get $\text{Tr}[(R_p^\dagger R_p)^{n/2}]$, with the result in (e), where the middle line contains n S^3 s.

As an exercise of these two properties, we have the factorization of a S^3 with more than one Wilson loops that do not link with each other, see (S30) as the two-loop case. The reason is that empty S^2 -tubes can be cut to separate the loops into different S^3 s.

The intuition behind (S11) is as follows. The partition function can be viewed as an inner product

$$Z(M) = \langle \psi_L | \psi_R \rangle, \quad (\text{S12})$$

when cutting the S^2 -tube, where $|\psi_L\rangle, |\psi_R\rangle$ are the left/right states on the cut interface S^2 . Since the Hilbert space of S^2 with one pair of anyons is one-dimensional, the two states $|\psi_L\rangle, |\psi_R\rangle$ simply differ by a complex number prefactor. On the other hand, a S^3 with a Wilson loop a is also an inner product $Z_a = \langle \psi_a | \psi_a \rangle$, where the state $|\psi_a\rangle$ lives in the same Hilbert space as $|\psi_L\rangle, |\psi_R\rangle$. Using this reference state, (S11) comes from the identity

$$\langle \psi_L | \psi_R \rangle \langle \psi_a | \psi_a \rangle = \langle \psi_L | \psi_a \rangle \langle \psi_a | \psi_R \rangle, \quad (\text{S13})$$

for any three states in an one-dimensional Hilbert space.

Before treating the general situation using surgery, we first warm up by calculating an example in full detail. Consider CCNR for Fig. 2(b) in the main text with fixed WL representation $|\psi\rangle = |a\rangle$. First, the torus under tripartition is deformed into the ball-tube system in Fig. S2(b), where three party balls are connected by D^2 -tubes in a circle. To trace over B and get ρ_A , we take the torus with its mirrored replica (with orientation and WL direction reversed), and glue the B regions together in Fig. S2(c). In the ball-tube representation for $|\psi\rangle$, this can be done

separately for each ball: The A_1A_2 ball just doubles with another $A'_1A'_2$, while the A_1B (A_2B similar) ball glues with a BA'_1 to produce a $A_1A'_1$ ball. After gluing the balls, it remains to glue the two tubes belonging to B : the result is one tube with cross section S^2 (two D^2 s glued together) that connects the interiors of $A_1A'_1$ and $A_2A'_2$. Next, we need to take n (even) copies of ρ_A and glue them such that the partition function yields $\text{Tr}[(R_\rho^\dagger R_\rho)^{n/2}]$ in the replica trick. In this case, it is convenient to align the n copies in a horizontal line (with periodic boundaries due to the trace), with the odd ones rotated in the paper by 180 degree. Then we just glue each copy to the part of its two neighbors that face towards it, as shown in Fig. S2(d). Still, we glue balls first before tubes. For all $p = 1, \dots, n/2$, the $A_1A'_1$ ($A_2A'_2$) ball of the $(2p)$ -th copy glues with that of the $(2p+1)$ -th ($(2p-1)$ -th) copy, which produces a S^3 . The n balls shared by the two parties (either A_1A_2 or $A'_1A'_2$), however, are glued in two disconnected groups where each group produces a S^3 . Finally, D^2 -tubes are glued in pairs to S^2 -tubes, while the S^2 -tubes connecting $A_1A'_1$ with $A_2A'_2$ remain, and we arrive at a complicated topology Fig. S2(e) with WLs threading inside. However, we can cut each S^2 -tube using (S11), and the price is just invoking an extra factor Z_a^{-1} . Furthermore, after the cut, there is one Wilson loop of representation a left in each S^3 . Since there are $3n$ S^2 -tubes and $n+2$ S^3 s, and the partition function of disconnected manifolds factorize, we have

$$\text{Tr}[(R_\rho^\dagger R_\rho)^{n/2}] = Z_a^{-3n} Z_a^{n+2} = Z_a^{2-2n} \rightarrow 1, \quad (\text{S14})$$

in the limit $n \rightarrow 1$, yielding $\mathcal{E}_{\text{CCNR}}^{\text{top}} = 0$.

We make two observations in the calculation above. First, each ball in $|\psi\rangle$ is glued with its replicas in a *local* way independent of the other balls/tubes. Second, we merely count the number of S^2 -tubes and S^3 s in the end, and it does not matter which S^3 is connected to which in the *global* topology. These also hold when the WL representation is not fixed. The rest of this section is to make these statements rigorous and derive results in the previous subsection.

B. no Wilson line

In this subsection we consider the case without WLs, and derive the first terms in (S6) and (S8). Treating WLs will be tedious, but shares the same basic idea in this subsection: each entanglement quantity in the replica method is (roughly) *product of local contributions* from individual balls.

Thanks to the symmetry $A_1 \leftrightarrow A_2$ in the problem, we classify the balls in \mathcal{B} to 4 types: $\mathcal{B}_A, \mathcal{B}_B, \mathcal{B}_{12}, \mathcal{B}_{AB}$ where the subscript indicates what parties the ball belongs to. For example, \mathcal{B}_A belongs to either A_1 or A_2 , while \mathcal{B}_{12} is an edge ball shared by A_1 and A_2 . Slightly abusing notation, we use (for example) \mathcal{B}_A to represent two precise items: 1. any ball of type \mathcal{B}_A , and 2. the set of all such balls. These 4 types are sketched in the first column of Table I, where $L, R \geq 0$ means the number of tubes going out of the left/right half-ball, although for $\mathcal{B}_A, \mathcal{B}_B$ only their sum $L+R$ is meaningful. We label the balls by β , so L, R are actually functions $L(\beta), R(\beta)$.

1. trace over B

For the entanglement measures we consider, the first manipulation on the state is always tracing B to get the density matrix ρ_A . Although it is sophisticated to plot the global geometry of the path-integral representation of ρ_A , it is clear what happens locally to each ball (together with its attached tubes), as shown in the second column of Table I. A \mathcal{B}_A or \mathcal{B}_{12} ball is just duplicated. A \mathcal{B}_{AB} becomes a ball composed of A and A' half-balls, and the tubes connecting B becomes tubes with cross section S^2 . A \mathcal{B}_B becomes a S^3 , with all its tubes becoming S^2 -tubes.

This last case actually yields the normalization of the state, where each ball is traced over as a whole to become S^3 . For one ball, it has $L+R$ S^2 -tubes. So in the surgery method, we should use $L+R$ balls to cut them, which yields a factor of Z^{-L-R} from (S11). Here $Z = \mathcal{S}_{00}$ is the partition function for a S^3 without WLs (S10). Since each tube is shared by two balls, each ball contributes $Z^{1-(L+R)/2}$ as a whole, where the Z^1 factor comes from the ball itself and the rest comes from the tubes attached to it. Then the normalization is

$$\langle \psi | \psi \rangle = \prod_{\beta \in \mathcal{B}} \alpha_1(\beta) = Z^{1-g}, \quad (\text{S15})$$

where we have defined

$$\alpha_n(\beta) := Z^{1-[L(\beta)+R(\beta)]n/2}, \quad (\text{S16})$$

for each ball β in the representation of $|\psi\rangle$. Observe that this result is determined *locally* by looking at the balls individually. It does not depend on which ball is connected to which. This is the key feature that enables all our calculations. Note that in this subsection $|\psi\rangle$ (and ρ_A etc) is the *unnormalized* state represented by path integral with no prefactors, unlike (S2).

(0,0)	$ \psi\rangle$	ρ_A	$\text{Tr}(\rho_A^n)$ or $\text{Tr}(\rho_A^{T_2})^n$	$\text{Tr}(R_\rho^\dagger R_\rho)^{n/2}$
\mathcal{B}_{AB}				
\mathcal{B}_{12}				
\mathcal{B}_A				
\mathcal{B}_B				

TABLE I. Local contribution of the four types of balls to various quantities, if there is no WL. We refer to the element in the second row, third column as (2,3) for example. The third column represents both EE and PT in the following way: we only show the PT value $\text{Tr}(\rho_A^{T_2})^n$ with n even for \mathcal{B}_{12} , because for EE it is the same as \mathcal{B}_A . For the other three types, EE and PT are literally the same, so one plot represents both. For the fourth column n is even. The symbols are defined by Fig. S1(c) together with the following: L, R means the number of tubes going out of the left/right half-ball, while only two of the tubes are explicitly shown. A double-line means a tube of cross section S^2 , while a double-lined circle means S^3 . α_n is defined in (S16), and the (4,2) element shows that the normalization factor for n copies of ρ_A is α_1^n .

2. replica method for EE and PT

Focusing on EE first, in the replica method n copies of ρ_A should connect cyclically. This can be done locally for each ball in ρ_A . In Table I(1,2), ρ_A of \mathcal{B}_{AB} consists A, A' as its half-balls, so the cyclic connection of n balls yields a single S^3 . The R S^2 -tubes for each copy of ρ_A are just replicated n times. Among the $2L$ D^2 -tubes of the p -th copy, the L of them connected to A' combine with those connected to A of the $(p+1)$ -th copy, making L S^2 -tubes. Thus there are totally $n(L+R)$ S^2 -tubes going out of the S^3 , as shown in Table I(1,3), which contributes a factor α_n (S16) to $\text{Tr}(\rho_A^n)$. \mathcal{B}_{12} is the same as \mathcal{B}_A for calculating EE, where the A' ball of the p -th copy of ρ_A combines with A of the $(p+1)$ -th copy to yield a S^3 . Their tubes combine to S^2 -tubes accordingly. Thus there will be n S^3 s, each has $L+R$ S^2 -tubes, as shown in Table I(3,3). Moreover, the contribution of \mathcal{B}_A is the same as its contribution α_1^n to normalization. \mathcal{B}_B is not involved in the contraction process, so it is just replicated n times, giving an identical result to \mathcal{B}_A . This is expected because of the symmetry $S_A = S_B$. In conclusion, the unnormalized $\text{Tr}(\rho_A^n)$ is

$$\text{Tr}(\rho_A^n) = \left(\prod_{\beta \in \mathcal{B}_{AB}} \alpha_n(\beta) \right) \left(\prod_{\beta \in \mathcal{B} - \mathcal{B}_{AB}} \alpha_1^n(\beta) \right), \quad (\text{S17})$$

and when canceling with the normalization (S15),

$$\frac{\text{Tr}(\rho_A^n)}{\langle \psi | \psi \rangle^n} = \prod_{\beta \in \mathcal{B}_{AB}} \frac{\alpha_n(\beta)}{\alpha_1^n(\beta)} = \prod_{\beta \in \mathcal{B}_{AB}} Z^{1-n} = Z^{E_B(1-n)}. \quad (\text{S18})$$

This leads to the first term in (S6a) by taking the replica limit.

PT is almost the same as EE, because the only difference is that A_1 and A_2 contract in opposite directions in the cycle. Thus $\mathcal{B}_{AB}, \mathcal{B}_A, \mathcal{B}_B$ contributes exactly the same local factor as for EE, since they locally cannot tell the relative direction of contraction. That is why we put EE and PT in one column in Table I, where the EE for \mathcal{B}_{12} contributes the same amount as \mathcal{B}_A , and the (2,3) element is for PT only. To get Table I(2,3), the A_1A_2 ball of the p -th copy contracts with the $A'_1A'_2$ balls of the $(p-1)$ -th and the $(p+1)$ -th. Since n is even for PT, the A_1A_2 ball of the odd copies combine with the $A'_1A'_2$ ball of the even copies to get one S^3 , while the A_1A_2 ball of the even copies combine with the $A'_1A'_2$ ball of the odd copies to get another S^3 . Each of the two S^3 s contributes a factor $\alpha_{n/2}$ because there are $(L+R)n/2$ S^2 -tubes. Summing up all balls, we have

$$\frac{\text{Tr}(\rho_A^{T_2})^n}{\langle \psi | \psi \rangle^n} = \left(\prod_{\beta \in \mathcal{B}_{AB}} \frac{\alpha_n(\beta)}{\alpha_1^n(\beta)} \right) \left(\prod_{\beta \in \mathcal{B}_{12}} \frac{\alpha_{n/2}^2(\beta)}{\alpha_1^n(\beta)} \right) = \left(\prod_{\beta \in \mathcal{B}_{AB}} Z^{1-n} \right) \left(\prod_{\beta \in \mathcal{B}_{12}} Z^{2-n} \right) = Z^{E_B(1-n) + (E-E_B)(2-n)}, \quad (\text{S19})$$

which leads to the first term in (S6b) by taking $n \rightarrow 1$.

3. replica method for CCNR

Consider contracting n copies of ρ_A for CCNR. For the $(2p+1)$ -th copy, A_1 (A'_1) regions connect to A'_1 (A_1) of the $(2p)$ -th copy, while A_2 (A'_2) regions connect to A'_2 (A_2) of the $(2p+2)$ -th copy. This can be done for the four types of balls in the similar way above, so here we just report the results in the fourth column of Table I. Summing up all balls, we have

$$\frac{\text{Tr}(R_\rho^\dagger R_\rho)^{n/2}}{\langle \psi | \psi \rangle^n} = \left(\prod_{\beta \in \mathcal{B}_{AB}} \frac{\alpha_{n/2}^2(\beta)}{\alpha_1^n(\beta)} \right) \left(\prod_{\beta \in \mathcal{B}_{12}} \frac{\alpha_{n/2}^2(\beta)}{\alpha_1^n(\beta)} \right) = \left(\prod_{\beta \in \mathcal{B}_{AB}} Z^{-n/2} \right) \left(\prod_{\beta \in \mathcal{B}_{12}} Z^{2-n} \right) = Z^{E_B(-n/2) + (E-E_B)(2-n)}, \quad (\text{S20})$$

which leads to the first term in (S6c) by taking $n \rightarrow 1$.

C. normalization with Wilson line: extra factor for party balls

In the previous subsection we omitted WLS (or in other words, setting $\psi_a(w) = \delta_{a0}$). With WL, the local nature still holds, so we only need to recalculate the balls that the WLS traverse, gather all local extra factors (LEFs) from the WL contribution, and multiply them together with the no-WL result. Then after a careful sum over representations, the final result is in the form of a global extra factor (GEF) multiplied by the no-WL result.

Since there are 4 types of balls and many ways for a WL to traverse a ball, we separate the discussion into two subsections: this and the next. In this subsection we warm up by focusing on the normalization of the state, where all regions r_j can be viewed as one party. The balls in \mathcal{M}_3 are then all party balls which can be viewed as \mathcal{B}_B . We will check the orthogonality of the basis in (S2), and derive results that will be useful in Section ID.

1. only one WL, which traverses each ball at most once

We first consider only $W = 1$ WL for now. The state is then

$$|\psi\rangle = \sum_a \psi_a |a\rangle = \sum_a \tilde{\psi}_a |\tilde{a}\rangle, \quad \text{where} \quad \tilde{\psi}_a = \frac{1}{\sqrt{\langle \tilde{a} | \tilde{a} \rangle}} \psi_a. \quad (\text{S21})$$

Here, unlike $|a\rangle$, $|\tilde{a}\rangle$ is the *unnormalized* state defined by the path integral with the a -independent prefactor $Z^{(g-1)/2}$ (see (S15)) that normalizes the no-WL state $|0\rangle = |\tilde{0}\rangle$.

If w punctures \mathcal{M} , it can shrink along its trajectory to be contained in one ball; otherwise w is a loop, which we assume traverses each ball at most once for now. Thus we have two possibilities $\mathcal{B}'_1, \mathcal{B}'_2$ for a ball that contains WL, as shown in the first column of Table II. Note that only tubes containing the WL are shown explicitly, since other tubes without WL do not contribute to LEF. For normalization $\langle \psi | \psi \rangle$, each ball combines with its replica to produce a S^3 , and the D^2 -tubes become S^2 -tubes. The representation is denoted by a and a' for the two replicas, and there is a *global* summation over them: $\langle \psi | \psi \rangle = \sum_{aa'} \tilde{\psi}_a \tilde{\psi}_{a'}^* \langle \tilde{a}' | \tilde{a} \rangle$, where $\langle \tilde{a}' | \tilde{a} \rangle$ is $\langle 0 | 0 \rangle$ times the product of all LEFs.

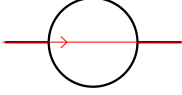
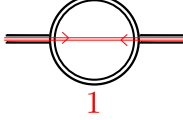
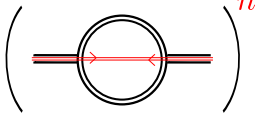
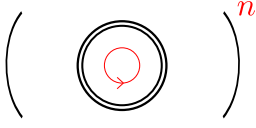
(0,0)	$ \psi\rangle$	$\langle\psi \psi\rangle$	$\text{Tr}(\rho_A^n)$ or $\text{Tr}(\rho_A^{T_2})^n$ or $\text{Tr}(R_\rho^\dagger R_\rho)^{n/2}$
\mathcal{B}'_1			
\mathcal{B}'_2			

TABLE II. LEF of a party ball traversed by one WL. Only the tubes containing the WL are shown.

For \mathcal{B}'_1 , each S^2 -tube traversed by the WL is cut by a S^3 with a Wilson loop in it, leaving another loop in the original S^3 . Since one loop can only have one representation, the surgery yields nonzero result only when $a = a'$, thus a factor $\delta_{aa'}$ should be included. Physically this is because the S^2 cross section of the tube hosts a Hilbert space, where excitation can only be created in anyon anti-anyon pairs. Since there are two tubes containing the WL together with the ball, the LEF is

$$Q^N(\mathcal{B}'_1) = \frac{Z_a^{1-2/2}}{Z^{1-2/2}} \delta_{aa'} = \delta_{aa'}, \quad (\text{S22})$$

where $Z_a = \mathcal{S}_{0a}$ is the partition function for a S^3 with an a -loop (S10), and $Z = Z_0$ is the $a = 0$ result. The superscript N refers to normalization.

For \mathcal{B}'_2 in the second row of Table II, the two WLs of the two replicas connect to form a loop in S^3 , which also requires $a = a'$. After cutting the tubes that all have no WL, the LEF is then

$$Q^N(\mathcal{B}'_2) = \frac{Z_a}{Z} \delta_{aa'} = d_a \delta_{aa'}, \quad (\text{S23})$$

where d_a is defined in (S7).

To sum up, the GEF of normalization due to WL is

$$\frac{\langle\psi|\psi\rangle}{\langle 0|0\rangle} = \sum_{aa'} \tilde{\psi}_a \tilde{\psi}_{a'}^* \delta_{aa'} \nu_a = \sum_a |\tilde{\psi}_a|^2 \nu_a \quad \text{where} \quad \nu_a := \begin{cases} 1, & \text{if } w \text{ is a loop} \\ d_a, & \text{if } w \text{ is not a loop} \end{cases} \quad (\text{S24})$$

Here “not a loop” means w punctures \mathcal{M} at two points. Thus in order for $|\psi\rangle$ to be normalized, we have

$$\tilde{\psi}_a = \psi_a \nu_a^{-1/2}. \quad (\text{S25})$$

2. multiple WLs, where each WL can traverse a ball multiple times

Now we consider the general case with $W > 1$ WLs, and each WL can traverse a ball more than once. If for each ball there is still at most one WL that passes it, then all balls' contribution to normalization is multiplied so that the total WL contribution factorizes to each individual WL. Formally, the GEF Q is

$$\begin{aligned} Q &= \sum_{a(1)a'(1)a(2)\dots a'(W)} \left(\prod_{w=1}^W \tilde{\psi}_{a(w)} \tilde{\psi}_{a'(w)}^* \right) \prod_{\beta \in \mathcal{B}} Q_\beta \\ &= \prod_{w=1}^W \left(\sum_{a(w)a'(w)} \tilde{\psi}_{a(w)} \tilde{\psi}_{a'(w)}^* \prod_{\beta \in \mathcal{B}} Q_\beta(w) \right), \end{aligned} \quad (\text{S26})$$

as long as the LEF for each ball factorizes

$$Q_\beta = \prod_{w=1}^W Q_\beta(w), \quad (\text{S27})$$

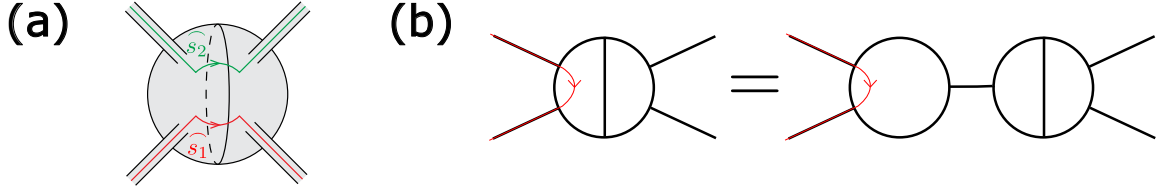


FIG. S3. (a) Example of two WLs traversing one ball. The WLs lie on the surface and do not intersect due to Assumption 2. As a consequence, the Wilson loops in the final S^3 do not link. (b) A WL in an edge ball that does not traverse the interface, is equivalent to the WL traversing a new party ball, i.e., \mathcal{B}'_1 in Table II.

where $Q_\beta(w)$ is the LEF if WLs other than w are all removed. (S27) is trivial if only one WL w passes β , because then $Q_\beta = Q_\beta(w)$ and $Q_\beta(w') = 1$ for $w' \neq w$. Moreover, if w traverses β $M(w, \beta)$ times, then the ball contains $M(w, \beta)$ segments of WL w . Intuitively, a ball locally cannot distinguish whether two WL segments in it belong to one WL or not, so we expect a further factorization similar to (S27):

$$Q_\beta(w) = \prod_{m=1}^{M(w, \beta)} Q_\beta(w, m), \quad (\text{S28})$$

where $Q_\beta(w, m)$ is the LEF when only the m -th segment of w is present.

Before proving (S27) and (S28), we first discuss their implication for normalization. A loop w may traverse a ball multiple times, but since $Q_\beta(w, m)$ is always $\delta_{aa'}$ (S22) whose power equals itself, the LEF $Q_\beta(w)$ is still $\delta_{aa'}$ as long as w traverses β . On the other hand, if w is not a loop, it is contained in one ball and we do not need (S28). As a result, the GEF is just the product of (S24) using (S27):

$$\frac{\langle \psi | \psi \rangle}{\langle 0 | 0 \rangle} = \prod_{w=1}^W \sum_a |\tilde{\psi}_a(w)|^2 \nu_a = \prod_{w=1}^W \sum_a |\psi_a(w)|^2. \quad (\text{S29})$$

This verifies that the basis in (S2) is orthogonal.

It remains to show (S27) and (S28), which combine to just one claim: the LEF for each ball factorizes to the WL segments contained in it. We prove this for two WL segments, since the general case follows similarly.

Suppose WL segments s_1 and s_2 traverse β as shown in Fig. S3(a), with representation a_1 and a_2 . They can belong to either one or two WLs globally. For the former case, there is a *global* prefactor $\delta_{a_1 a_2}$, but that is irrelevant for LEF here. According to Assumption 2, the two WL segments live on the surface of the ball, and each D^2 -tube contains at most one WL segment. On the ball, the two ‘‘arcs’’ \widehat{s}_1 and \widehat{s}_2 do not touch each other. Then it is clear that after gluing replicas and cutting the S^2 -tubes, the remaining Wilson loops for s_1 and s_2 in the S^3 do not link with each other. Its partition function $Z_{a_1 a_2}$ is then factorized due to the surgery operation in Fig. S2 with WL in the tube

$$Z_{a_1 a_2} \cdot Z = Z_{a_1} Z_{a_2}, \quad \implies \quad \frac{Z_{a_1 a_2}}{Z} = \frac{Z_{a_1}}{Z} \frac{Z_{a_2}}{Z}. \quad (\text{S30})$$

On the other hand, LEF due to cutting tubes (which includes factors like $\delta_{a_1 a'_1}$) also factorizes because each S^2 -tube belongs to either s_1 or s_2 , or neither. This establishes the factorization properties (S27) and (S28).

D. Wilson line contribution to entanglement

In this subsection, we derive the GEF for the three entanglement measures at any replica number n , which reduces to our main results (S6) and (S8) by combining with the results in Section IB and taking special limits. Again, we first consider a state (S21) with $W = 1$ WL, which is assumed to traverse each ball at most once. We use the factorization property to handle the general case in the final subsection.

1. WL in an edge ball that traverses the interface

There are totally seven possibilities for the WL to traverse the interface of an edge ball, as shown by $\tilde{\mathcal{B}}_1, \dots, \tilde{\mathcal{B}}_7$ in the first column of Table III. Recall that only tubes containing the WL are shown explicitly. As in Section IB, we first trace over B to get ρ_A , as shown in the second column.

We move on to EE and PT. As discussed in Section IB, for these two quantities the local contraction structure is the same for \mathcal{B}_{AB} , while for \mathcal{B}_{12} we only need to consider PT. Thus we report the results in the single third column in Table III. Taking $\tilde{\mathcal{B}}_1$ for example, n copies of ρ_A contract to one S^3 with n S^2 -tubes on both sides. Each of the n tubes on the left comes from the S^2 -tube of one copy. For the right, the D^2 -tube with a'_p -line of the p -th copy combine with the D^2 -tube with a_{p+1} -line of the $(p+1)$ -th copy to yield one S^2 -tube, where $p = 1, \dots, n$. In this process all representations are identified to a , which yields a factor

$$[11' \cdots nn'] := \delta_{a_1 a'_1} \delta_{a'_1 a_2} \delta_{a_2 a'_2} \cdots \delta_{a_n a'_n}. \quad (\text{S31})$$

Hereafter we use such shorthand notations to identify all representations in the square brackets. Furthermore, along the WLs one can traverse all of the $2n$ S^2 -tubes if hopping between the two lines in one tube is allowed. This means when cutting all the tubes in surgery, there is only one loop of representation $a_1 \equiv a$ left in the S^3 . Since each S^2 -tube is cut by a S^3 with an a -loop, the LEF is then

$$Q^{\text{EE}}(\tilde{\mathcal{B}}_1) = Q^{\text{PT}}(\tilde{\mathcal{B}}_1) = \frac{Z_a^{1-2n/2}}{Z^{1-2n/2}} [11' \cdots nn'] = d_a^{1-n} [11' \cdots nn']. \quad (\text{S32})$$

The other cases are worked out similarly, for example

$$Q^{\text{PT}}(\tilde{\mathcal{B}}_5) = d_{a_1}^{1-n/2} d_{a_2}^{1-n/2} \times [12' \cdots (n-1)n'] \times [1'2 \cdots (n-1)n]. \quad (\text{S33})$$

CCNR is similar, for which we report the result for all types of balls in the fourth column of Table III. There are three possibilities locally for which representations are equal: \mathcal{B}_{12} has (S33), while \mathcal{B}_{1B} and \mathcal{B}_{2B} yield

$$[11'22'] \times [33'44'] \times \cdots \times [(n-1)(n-1)'nn'], \quad (\text{S34})$$

and

$$[22'33'] \times [44'55'] \times \cdots \times [nn'11'], \quad (\text{S35})$$

respectively. For example,

$$Q^{\text{CCNR}}(\tilde{\mathcal{B}}_1) = \prod_{p=1}^{n/2} d_{a_{2p-1}}^{-1} \times (\text{either (S34) or (S35)}), \quad (\text{S36})$$

depending on whether the left half-ball is A_1 or A_2 . Note that PT and CCNR are identical for \mathcal{B}_{12} , which is also manifest in Table I.

2. WL in a party ball

For a party ball, it can be traversed by the WL in two ways $\mathcal{B}'_1, \mathcal{B}'_2$ as shown in Table II. There is no WL segment that goes through one tube and punctures the ball surface once, because it can shrink to disappear in this ball. For each of the two cases at a given replica number n , the final topology is the same regardless of the entanglement measure and the party (A_1, A_2 or B) of the ball, which is already manifest in Table I. As shown in the third column of Table II, it is just n disconnected copies of the $n=1$ topology for normalization. The identification of representations, however, depends on the party. We first focus on B . Using (S22) and (S23), the LEFs are

$$Q(\mathcal{B}'_1) = [11'] \times [22'] \times \cdots \times [nn'], \quad \text{for } \mathcal{B}_B \quad (\text{S37})$$

and

$$Q(\mathcal{B}'_2) = \prod_{p=1}^n d_{a_p} \times [11'] \times [22'] \times \cdots \times [nn'], \quad \text{for } \mathcal{B}_B. \quad (\text{S38})$$

Since \mathcal{B}'_2 contains the whole WL, the GEF for any entanglement measure is then

$$\sum_{a_1 a'_1 \cdots a'_n} \tilde{\psi}_{a_1} \tilde{\psi}_{a'_1}^* \cdots \tilde{\psi}_{a_n} \tilde{\psi}_{a'_n}^* Q(\mathcal{B}'_2) = \left(\sum_a |\tilde{\psi}_a|^2 d_a \right)^n = 1, \quad (\text{S39})$$

(0,0)	$ \psi\rangle$	ρ_A	$\text{Tr}(\rho_A^n)$ or $\text{Tr}(\rho_A^{T_2})^n$	$\text{Tr}(R_\rho^\dagger R_\rho)^{n/2}$		
$\tilde{\mathcal{B}}_1$					d_a^{1-n}	
$\tilde{\mathcal{B}}_2$			[11'...nn']		d_a^{1-n}	
$\tilde{\mathcal{B}}_3$						$d_a^{1-\frac{n}{2}} = d_a^{\frac{n}{2}} \cdot d_a^{1-n}$
$\tilde{\mathcal{B}}_4$						$d_a = d_a^n \cdot d_a^{1-n}$
$\tilde{\mathcal{B}}_5$			[12'3...n'] \times [1'23'...n]		$\prod_{p=1}^{n/2} d_{a_{2p-1}}^{-1}$	
$\tilde{\mathcal{B}}_6$						$\prod_{p=1}^2 d_{a_p}^{1-\frac{n}{4}} = \prod_{p=1}^2 d_{a_p}^{\frac{n}{4}} d_{a_p}^{1-\frac{n}{2}}$
$\tilde{\mathcal{B}}_7$						$\prod_{p=1}^2 d_{a_p} = \prod_{p=1}^2 d_{a_p}^{\frac{n}{2}} d_{a_p}^{1-\frac{n}{2}}$

TABLE III. LEF for various quantities for the 7 types of balls $\tilde{\mathcal{B}}_1, \dots, \tilde{\mathcal{B}}_7$. See Table I on how EE and PT are combined. The LEF depends on both the topology of the final object (the fourth and fifth column), and the way representations are identified, which yields a factor (defined by e.g. (S31)) shown in the third and last column. The symbols are the same as Fig. S1(c) and Table I, and the crossing structure of WLS indicates that each S^3 contains exactly one Wilson loop after cutting the S^2 -tubes.

using (S25). This result is intuitive: the WL is created locally in the single region, so it does not affect the entanglement among regions. (S39) actually holds for all parties, because the representations are always identified in prime and no-prime pairs.

On the other hand, the party also does not matter for \mathcal{B}'_1 , because we can always set $Q(\mathcal{B}'_1) = 1$ without changing the product of all LEFs (which yields GEF after summing over representations). The reason is that for a WL in \mathcal{B}'_1 , it must traverse the interface of another edge ball, whose LEF already includes the representation-identification factor of the party ball. For example, if the party ball is \mathcal{B}_B , then the WL must traverse the interface of another \mathcal{B}_{AB} : otherwise it can shrink to be contained in the party ball. Then the LEF for \mathcal{B}_{AB} includes a factor either (S31), (S34) or (S35), which all has (S37) as a factor.

3. WL in an edge ball that does not traverse the interface

The only case missing in the previous analysis is that the WL traverses an edge ball, but not through its interface: it goes in and out of the same half-ball. As shown in Fig. S3(b), this case actually reduces to \mathcal{B}'_1 when separating the ball into two balls: an edge ball with no WL and a party ball that the WL traverses. Thus according to the previous subsection, the LEF can be set to 1.

4. GEF for only one WL, which traverses each ball at most once

The previous three subsections discuss all cases assuming there is only one WL, and it traverses each ball at most once. We see that as long as the WL is not contained in a single region where the GEF is trivial (S39), we only need to consider the cases in Table. III by setting all other LEFs to 1.

Summing up the \mathcal{B}_{AB} cases in the third line of Table III, we get the GEF for EE

$$\begin{aligned} \frac{\text{Tr}(\rho_A^n)}{\text{Tr}(\rho_A^n)_0} &= \sum_{a_1 a'_1 \dots a_n a'_n} \tilde{\psi}_{a_1} \tilde{\psi}_{a'_1}^* \dots \tilde{\psi}_{a_n} \tilde{\psi}_{a'_n}^* [11' \dots nn'] \prod_{\beta \in \tilde{\mathcal{B}}_1} d_a^{1-n} \prod_{\beta \in \tilde{\mathcal{B}}_2 \cup \tilde{\mathcal{B}}_3} d_a^{1-n/2} \prod_{\beta \in \tilde{\mathcal{B}}_4} d_a \\ &= \sum_a |\psi_a|^{2n} \nu_a^{-n} \prod_{\beta \in \tilde{\mathcal{B}}_1} d_a^{1-n} \prod_{\beta \in \tilde{\mathcal{B}}_2 \cup \tilde{\mathcal{B}}_3} d_a^{1-n/2} \prod_{\beta \in \tilde{\mathcal{B}}_4} d_a = \sum_a |\psi_a|^{2n} d_a^{(1-n)K_B}, \end{aligned} \quad (\text{S40})$$

regardless of whether w is a loop or not. Here the subscript 0 means the normalized no-WL result, and we have used $[11' \dots nn']^2 = [11' \dots nn']$ together with (S25). The difference among $\tilde{\mathcal{B}}_1, \dots, \tilde{\mathcal{B}}_4$ turns out to cancel exactly with the normalization difference, which also holds for $\tilde{\mathcal{B}}_5, \tilde{\mathcal{B}}_6, \tilde{\mathcal{B}}_7$ and for PT and CCNR as we will see. (S40) leads to the second term in (S6a) by taking the limit

$$\lim_{n \rightarrow 1} \frac{1}{1-n} \log \left(\sum_a x_a^n y_a^{1-n} \right) = \sum_a x_a (\log y_a - \log x_a), \quad \text{if } \sum_a x_a = 1. \quad (\text{S41})$$

For PT, we have two possibilities on whether w traverses a \mathcal{B}_{AB} or not. If $K_B > 0$, all representations $a_1, a'_1, \dots, a_n, a'_n$ are equal due to the factor (S31) from one of the \mathcal{B}_{AB} ; otherwise they are equal in two disjoint groups with prefactor (S33) due to \mathcal{B}_{12} . The GEF for PT is then

$$\frac{\text{Tr}(\rho_A^{T_2})^n}{\text{Tr}(\rho_A^{T_2})_0^n} = \begin{cases} \sum_a |\psi_a|^{2n} d_a^{(1-n)K_B} d_a^{(2-n)(K-K_B)}, & K_B > 0 \\ \left(\sum_a |\psi_a|^n d_a^{(1-n/2)(K-K_B)} \right)^2, & K_B = 0 \end{cases} \quad (\text{S42})$$

For CCNR, since any two of (S33), (S34) and (S35) multiply to (S31), there are also three possibilities for the global prefactor: Among the three quantities K_{12}, K_{1B}, K_{2B} , if at least two are non-zero then the prefactor is (S31); if only K_{1B} or K_{2B} is non-zero the prefactor is (S34) (which is equivalent to (S35)); finally if only $K_{12} > 0$ the prefactor is (S33). To summarize, the GEF for CCNR is

$$\frac{\text{Tr}(R_\rho^\dagger R_\rho)^{n/2}}{\text{Tr}(R_\rho^\dagger R_\rho)_0^{n/2}} = \begin{cases} \sum_a |\psi_a|^{2n} d_a^{-nK_B/2} d_a^{(2-n)(K-K_B)}, & \text{if at least two in } \{K_{12}, K_{1B}, K_{2B}\} \text{ are nonzero} \\ \left(\sum_a |\psi_a|^4 d_a^{-K_B} \right)^{n/2}, & \text{if only one in } \{K_{1B}, K_{2B}\} \text{ is nonzero and } K_{12} = 0 \\ \left(\sum_a |\psi_a|^n d_a^{(1-n/2)(K-K_B)} \right)^2, & K_B = 0 \end{cases} \quad (\text{S43})$$

5. general case: factorization property

Although Section IC only focuses on normalization, the factorization property of LEF in (S27) and (S28) generally holds for all three entanglement measures, at any replica number n . The LEFs by cutting S^2 -tubes are factorized simply due to Assumption 2 where at most one WL is contained in each D^2 -tube. On the other hand, the LEF of Wilson loops in an S^3 generated by gluing \tilde{n} balls is also factorized (Section IC being the $\tilde{n} = 2$ case), because the loops do not link so that (S30) follows. The absence of linking is guaranteed because WLs do not touch on the surface of the ball, so they are in “different continents” in the S^3 .

Thanks to such factorization, the GEFs (S40),(S42) and (S43) hold even if the WL traverses a ball more than once. This is justified by the following two observations. First, the different situations (lines) in (S42) and (S43) only depend on whether each K quantity (K, K_P or $K_{PP'}$) is zero or not. Thus traversing a ball more than once does not change the zeroness of the K s, so the situation (line) is unchanged. Second, the exponents of the power of d_a in (S40),(S42) and (S43) are all proportional to K s. This agrees with the factorization property, because traversing an interface one more time just adds one to the corresponding K . Finally, multiple WLs also factorize due to (S27), so each WL contributes by (S40),(S42) and (S43), while all WLs are summed over in the end. This completes our derivation for (S6) and (S8).

II. ENTANGLEMENT MEASURES IN STABILIZER FORMALISM

A. CCNR in stabilizer formalism

For each $g \in G_A$, we can write $g = O^{A_1} \otimes O^{A_2}$ such that O^{A_i} acts on subsystem A_i and is a Pauli operator up to a sign. We then have

$$\text{Tr} [(R^\dagger R)^m] = \frac{1}{2^{2mn_A}} \sum_{g_1, \dots, g_{2m} \in G_A} \prod_{i=1}^m \text{Tr}(O_{2i-1}^{A_1} O_{2i}^{A_1}) \text{Tr}(O_{2i}^{A_2} O_{2i+1}^{A_2}) \quad (\text{S44})$$

where $g_i = O_i^{A_1} \otimes O_i^{A_2}$. The summand above is nonzero if and only if $O_{2i-1}^{A_1} \propto O_{2i}^{A_1}$ and $O_{2i}^{A_2} \propto O_{2i+1}^{A_2}$ for all i (identifying $2m+1$ and 1). We then only need to consider the case where $y_{2i-1,2i} := g_{2i-1} g_{2i} \in G_{A_2}$ and $x_{2i,2i+1} := g_{2i} g_{2i+1} \in G_{A_1}$. The summation over g_1, \dots, g_{2m} in Eq. S44 can then be replaced with a summation over $g_1, x_{2i,2i+1}$, and $y_{2i-1,2i}$. Note that the x 's and y 's are not all independent: Since $g_2 = g_1 y_{12}, g_3 = g_2 x_{23}, \dots$, we have $g_1 = g_1 y_{12} x_{23} y_{34} \dots y_{2m-1,2m} x_{2m,1}$, and thus

$$y_{12} y_{34} \dots y_{2m-1,2m} = 1, \quad x_{23} x_{45} \dots x_{2m,1} = 1. \quad (\text{S45})$$

Let \sum' be the sum over the independent variables $g_1 \in G_A, x_{23}, \dots, x_{2m-2,2m-1} \in G_{A_1}$, and $y_{12}, \dots, y_{2m-3,2m-2} \in G_{A_2}$. We have

$$\text{Tr} [(R^\dagger R)^m] = \frac{1}{2^{2mn_A}} \sum' \text{Tr}_{A_1}(1)^m \text{Tr}_{A_2}(1)^m = 2^{k+(m-1)(k_1+k_2)-mn_A}, \quad (\text{S46})$$

where k_1 and k_2 are the number of generators of G_{A_1} and G_{A_2} , respectively. Taking the limit $m \rightarrow 1/2$, we obtain the CCNR negativity:

$$\mathcal{E}_{\text{CCNR}} = k - \frac{1}{2}(k_1 + k_2) - \frac{1}{2}n_A = \frac{1}{2}(S_{A_1}^{(\alpha)} + S_{A_2}^{(\alpha)}) - S_A^{(\alpha)}. \quad (\text{S47})$$

B. PT in stabilizer formalism

As mentioned in the main text, we have the following canonical choice of the generators of G_{12} :

$$G_{12} = \langle z_1, \dots, z_r, w_1, \dots, w_s, \bar{w}_1, \dots, \bar{w}_s \rangle, \quad (\text{S48})$$

such that $p_{A_2}(z_i)$ commutes with all generators of G_{12} , and $p_{A_2}(w_i)$ commutes with all generators of G_{12} except for \bar{w}_i . Now we can write the reduced density matrix ρ_A as

$$\rho_A = \frac{1}{2^{n_A}} \sum_{g \in G_{A_1}} \sum_{g' \in G_{A_2}} \sum_{h \in G_{12}} gg'h. \quad (\text{S49})$$

Let U and V be two stabilizers, we generally have $(UV)^{T_2} = \pm U^{T_2} V^{T_2}$ when $p_{A_2}(U)$ and $p_{A_2}(V)$ commute (anticommute). We therefore have

$$\text{Tr} [(\rho_A^{T_2})^m] = \frac{1}{2^{mn_A}} \sum_{\{g_i, g'_i, h_i\}} \text{Tr} [(g_1 \dots g_m)(g'_1 \dots g'_m)^{T_2}(h_1^{T_2} \dots h_m^{T_2})], \quad (\text{S50})$$

where $g_i \in G_{A_1}$, $g'_i \in G_{A_2}$, and $h_i \in G_{12}$. The sums over g and g' can now be performed with the constraints $g_1 \cdots g_m = g'_1 \cdots g'_m = 1$, and we obtain

$$\mathrm{Tr} \left[(\rho_A^{T_2})^m \right] = \frac{2^{(m-1)(k_1+k_2)}}{2^{mn_A}} \sum_{\{h_i\}} \mathrm{Tr}(h_1^{T_2} \cdots h_m^{T_2}). \quad (\text{S51})$$

Since the effect of partial transpose on a stabilizer is just a \pm sign, for the trace on the right-hand side to be nonzero, we must have $h_m = h_1 \cdots h_{m-1}$. The difficult part is to figure out the sign of this trace. Each $h_i \in G_{12}$ can be expanded as a product of the canonical generators, and is thus represented by a collection of \mathbb{Z}_2 indices $(\lambda_1^i, \dots, \lambda_r^i, \mu_1^i, \dots, \mu_s^i, \nu_1^i, \dots, \nu_s^i)$, corresponding to the powers of z_i , w_i , and \bar{w}_i , respectively. We define an operator \tilde{h}_i , by replacing each canonical generator in the expansion of h_i by its partial transpose. For example, if $h_i = z_a w_b \bar{w}_c$, then $\tilde{h}_i = z_a^{T_2} w_b^{T_2} \bar{w}_c^{T_2}$. Notice that $h_1 h_2 \cdots h_m = 1$ implies $\tilde{h}_1 \tilde{h}_2 \cdots \tilde{h}_m = 1$ as well. One can see that $h_i^{T_2} = \tilde{h}_i \exp(i\pi \sum_l \mu_l^i \nu_l^i)$. The sign of $\mathrm{Tr}(h_1^{T_2} \cdots h_m^{T_2})$ is then given by

$$\prod_{l=1}^s \exp \left\{ i\pi \left[- \sum_{i=1}^{m-1} \mu_l^i \nu_l^i + \left(\sum_{i=1}^{m-1} \mu_l^i \right) \left(\sum_{j=1}^{m-1} \nu_l^j \right) \right] \right\}. \quad (\text{S52})$$

The summation over ν_l^i gives nonzero result only if any $(m-2)$ elements of $\{\mu_l^1, \dots, \mu_l^{m-1}\}$ sum up to an even integer. For the case of even m , this implies that $\mu_l^1, \dots, \mu_l^{m-1}$ are either all even or all odd. The independent variables to sum over are therefore μ_l^1 for all l , and ν_l^i for $i = 1, \dots, m-1$ and all l . Also remembering that $\mathrm{Tr}_A(1) = 2^{n_A}$, we finally arrive at the result

$$\sum_{\{h_i\}} \mathrm{Tr}(h_1^{T_2} \cdots h_m^{T_2}) = 2^{ms+n_A} \quad (m \text{ even}). \quad (\text{S53})$$

Taking the limit $m \rightarrow 1$, we obtain

$$\mathcal{E}_{\mathrm{PT}} = s = \frac{1}{2}(k - k_1 - k_2 - r) = \frac{1}{2}I^{(\alpha)}(A_1, A_2) - \frac{1}{2}r, \quad (\text{S54})$$

where $I^{(\alpha)}(A_1, A_2)$ is the Renyi mutual information, and r is defined in Eq. S48.

The result above implies that when $\mathcal{E}_{\mathrm{PT}} < I^{(\alpha)}(A_1, A_2)/2$, there is a stabilizer $g \in G_A$ whose restriction to A_2 commutes with G_A but does not belong to G_{A_2} (up to an ambiguous sign). The reverse is in fact also true. Supposing such a stabilizer g exists, it does not belong to $G_{A_1}G_{A_2}$, and thus can be extended to a set of generators defining G_{12} . As we mentioned in the main text, it is always possible to choose the signs of $p_{A_2}(\cdot)$ such that $p_{A_2}(G_{12})$ forms a group, with r being the rank of its center. $p_{A_2}(g)$ commuting with G_A implies $r \geq 1$, and therefore $\mathcal{E}_{\mathrm{PT}} < I^{(\alpha)}(A_1, A_2)/2$. We have proved the following convenient result.

Corollary 1. *For a stabilizer state, $\mathcal{E}_{\mathrm{PT}}(A_1, A_2) \leq I^{(\alpha)}(A_1, A_2)/2$ for any α , with equality if and only if the following condition holds: There does not exist a stabilizer $g \in G_A$ whose restriction to A_2 commutes with G_A but does not belong to G_{A_2} (up to an ambiguous sign).*

C. one more toric code example

Consider the \mathbb{Z}_2 TC model on torus – square lattice with periodic boundary condition, and the tripartition in Fig. 2(b) of the main text: A_1 and A_2 are adjacent, and all interface circles are vertical. The TC Hamiltonian has four degenerate ground states, so we need to specify two more stabilizers besides the star and plaquette terms. The TC model has two independent types of string operators: the e string consisting of Pauli X operators along links, and the m string consisting of Pauli Z operators along dual lattice links. We consider the interesting situation where the additional stabilizers are *horizontal* e and m loops that wind around the torus. Each circular interface is crossed by the e or m loop once.

In a general CS theory, the state $|R_0\rangle$, defined by path integral inside the torus with no WL insertion, is an eigenstate with eigenvalue d_a of the vertical string/WL operator in the representation R_a , as one can verify using surgery. Hence, in the TC model, $|R_0\rangle$ is the eigenstate with eigenvalue $+1$ for both the *vertical* e and m loops. The state $|\psi\rangle$ we consider is then related to $|R_0\rangle$ by a modular \mathcal{S} transformation, or more precisely $|\psi\rangle = \sum_j \psi_j |R_j\rangle$, with

$\psi_j = \mathcal{S}_{0j} = 1/2$ ($j = 0, 1, 2, 3$), where we used $\mathcal{S}_{0j} = d_j/\mathcal{D}$ and $d_j = 1$, $\mathcal{D} = 2$. From our continuum results in the main text,

$$\text{(continuum)} \quad \mathcal{E}_{\text{CCNR}}^{\text{top}} = 0, \quad \mathcal{E}_{\text{PT}}^{\text{top}} = -1, \quad (\text{S55})$$

where the base of logarithm has been set to 2. The topological EE of A_1 , A_2 , or A is simply zero; this is the maximally entangled state.

Now let us get onto the lattice. We proposed in the main text that the following quantities are topological and universal:

$$\Delta_{\text{CCNR}} := \mathcal{E}_{\text{CCNR}}(A_1, A_2) + S_A^{(2)}/2 - \left[S_{A_1}^{(1/2)} + S_{A_2}^{(1/2)} - S_A^{(1/2)} \right] /2, \quad (\text{S56})$$

$$\Delta_{\text{PT}} := \mathcal{E}_{\text{PT}}(A_1, A_2) - \left[S_{A_1}^{(1/2)} + S_{A_2}^{(1/2)} - S_A^{(1/2)} \right] /2. \quad (\text{S57})$$

One can compute $\mathcal{E}_{\text{CCNR}}^{\text{top}}$ and $\mathcal{E}_{\text{PT}}^{\text{top}}$ by adding a superscript “top” to each term on the right-hand side of each equation above (and plugging in, say, the continuum results of topological EEs). From our results in the main text, $\Delta_{\text{CCNR}} = 0$, and $\Delta_{\text{PT}} = -r/2$. Since all topological EEs are zero for the state being considered, we see that the lattice result of $\mathcal{E}_{\text{CCNR}}^{\text{top}}$ matches with the continuum one. The lattice result of $\mathcal{E}_{\text{PT}}^{\text{top}}$ is $-r/2$. It is not hard to see $r = 2$ in this case: We can take z_1 (z_2) to be the product of two vertical e (m) loops inside A_1 and A_2 , respectively. A pair of vertical e (m) loops can be generated by the plaquette (star) terms in between and is indeed a valid stabilizer, but a single vertical e (m) loop anticommutes with the horizontal m (e) loop and does not belong to the stabilizer group. We have thus also verified $\mathcal{E}_{\text{PT}}^{\text{top}} = -1$ on the lattice.